VIETNAM NATIONAL UNIVERSITY OF FORESTRY

FOREST RESOURCES & ENVIRONMENTAL MANAGEMENT FACULTY

STUDENT THESIS

DETERMINING SUITABLE IMAGE CLASSIFICATION METHOD FOR MANGROVE FOREST IN NINH BINH PROVINCE WITH LANDSAT-8 OLI/TIRS AND SENTINEL-2 MSI SATELLITE IMAGERY

Major: Natural Resources Management

Code: D850101

Faculty: Forest Resources and Environmental Management

Student: Ho Manh Nhat Truong   **Student ID**: 1553090233

Class: K60-Natural Resources Management   **Course**: 2015-2019

Supervisor: Assoc. Prof., PhD. Tran Quang Bao

2019

ACKNOWLEDGEMENT

This research was conducted regarding the graduation requirement at Vietnam National University of Forestry (VNUF) for final thesis paper.

During the period of the research, I would like to show great appreciation to Assoc. Prof., PhD Tran Quang Bao for supervising and providing valuable guidance for my thesis paper and other friends who helped support intensive fieldwork and revise my paper with utmost attitude.

Also, the research would not be possible without the consent of the People's Committee of Kim Son district in Ninh Binh province for its permission to conduct field work at mangrove forest and support from the Department of Forest Protection in Kim Trung commune during my study there.

TABLE OF CONTENTS

ABBREVIATION

EM	Emitted Electromagnetic
EROS	Earth Resources Observation and Science
FAO	Food and Agriculture Organization
GIS	Geographic Information System
JRC	Japanese Red Cross
LULC	Land Use & Land Cover
MSI	Multi-spectral Instrument
NDVI	Normalized Difference Vegetation Index
NIR	Near Infrared
OBC	Object-based Classification
OLI	Operational Land Imager
RE	Remote Sensing
SWIR	Shortwave Infrared
TIRS	Thermal Infrared Sensors
UNEP	United Nations Environmental Program

LIST OF FIGURES

LIST OF TABLES

CHAPTER 1 : INTRODUCTION

Trees and shrubs in the tropical and subtropical coastal areas forming a unique saline woodland or shrubland habitat which can be termed as mangrove forests (Md. Mijanur Rahmana, 2013). The coastal forests contribute greatly to the primary productivity and economic development with valuable ecosystem goods, such as: firewood, fish, construction materials and so on (Primavera, 2000). Additionally, mangroves play an important role in bio-protection from coastal erosion, tropical storm, tsunami and so on (Phan Minh, 2007). Global warming trend is also mitigated by the carbon sink from mangrove forest area.

However, mangrove ecosystems have become one the world's most threatened biomes in the past half-century (Field, et al., 1998) with a 35% of reduction globally in the recent decades. The decreasing trend can be derived from anthropogenic activities, such as aqua-culture, agriculture, forest extraction and logging, and urban development as primary driving forces. In addition to human activities, natural events such as tsunamis, strong waves, tropical storms, etc. have also contributed to this loss. In the near future, the mangrove loss is expected to continue due to sea-level rise and climate change; and increase in human population along the coastal line (Mavis, 2001) (Gilman, Ellison, & Duke, 2008).Thus, it is essential for any government to facilitate plans and strategy to better monitor and conserve the valuable mangrove forest area.

Remote sensing has been proven to be greatly efficient in monitoring and mapping threatened mangrove ecosystems which can be shown by various studies carried out around the world (Claudia Kuenzer, 2011). Important information about habitat inventories, change detection and monitoring, ecosystem evaluation, productivity assessment, field survey planning of mangrove forests can be provided by remote sensing technology application on mangroves.

Understanding the usefulness of mangrove forests, Vietnam is one of the countries that have been trying to better conserve mangrove forests in recent years. Throughout the history, Vietnam has experienced a severe loss of mangrove forest area due to change of land uses and poor policies management (Thuy Dang Truong, 2018) With the advanced application of

remote sensing, various techniques are provided from many satellite systems to improve the efficiency in monitoring mangrove forests (LU & WENG, 2007).

It is essential to note that no universal choice of classification method and satellite data has been given for mapping mangrove forest (Congalton, 2001) (Hankui K. Zhanga, 2018) (Heumann B. W., 2011). However, for moderate spatial extents, delineating different mangrove communities/zones from high-resolution aerial photography and validation by ground-referencing provide the best resolution and accuracy (Manson, 2001). Despite the obvious advantages of remote sensing use, it can be costly to acquire timely high-resolution satellite imagery. Landsat-8 Operational Land Imager (OLI), Sentinel 2 Multi -Spectral Instrument (MSI) have provided a convenient and free access to medium and high spatial resolution images to monitor mangrove forests (Hu, 2013).

The relatively coarser spatial resolution images are usually well-suited with the traditional classification approaches based on statistical analysis of individual pixels (L. Wang, 2004). While it is predicted that high resolution images will improve the accuracy of pixel-based classification method, discrimination of land cover types usually requires a coarser scale. The number of detectable sub-classes increase corresponding with finer resolution makes it more difficult to discriminate spectrally mixed land cover types (Shaban, 2001). Object-based classification approaches, on the other hand, provide a promising mean to utilize other spatial information focusing on true meaning patterns of an object rather than similar pixels (Blaschke, 2001).

The result of classification process varies significantly corresponding to the features of study site (Young, 2017). Differentiation of boundaries can be limited by the capacity to discriminate scattered mangroves or clusters of trees that can occur along coastal lines (Manson, 2001) (Heumann B. W., 2011), particularly in Ninh Binh province where small and sparse canopy mangrove population is the main feature of northern provinces in Vietnam due to the large temperature variation among seasons and lower annual precipitation (Phan Nguyen Hong T. V., 1999).

Tidal regime is a significant factor that reduce accuracy in mapping mangroves using remote sensing techniques (Kerrylee Rogers, 2017). The absence and presence of sea water under the mangrove forest canopy can alter the reflectance significantly, complicating the

discrimination at a single tidal stage (Manson, 2001) (Kuenzer, 2011). The exploitation of mangrove zones at different tidal stages combination images will potentially improve the accuracy of the classification, compared with the standard approaches that classify single satellite scene (Kerrylee Rogers, 2017).

The aim of this study is to determine the suitable classification methods of mangrove forests in Ninh Binh province with free satellite imagery.

CHAPTER 2 : LITERATURE REVIEW

2.1 GIS and Remote sensing

2.1.1 *Concept of GIS and Remote sensing*

The term Geographical Information System (GIS) is used in geographically oriented computer technology that integrate systems in substantive applications or generation of massive interest worldwide (Paul A Longley, 2005).

Remote sensing (RS) is generally termed as the science and practice of acquiring information about an object without actual travel to it by sampling reflected and emitted electromagnetic (EM) radiation from Earth's terrestrial and aquatic ecosystems and atmosphere (Horning, 2008). Spectral, spatial, temporal and polarization signatures are the main characteristics of the sensor/target, which facilitate target discrimination of earth surface data as seen by sensors in different wavelengths. With the ability for a synoptic view, repetitive coverage with calibrated sensors to detect changes, observations at different resolutions, RS data provides a better alternative for natural resources management as compared to traditional methods. RS data is widely used in some major operational application themes, such as: forestry, agriculture, water resources, land use, geology, environment, coastal zones, marine monitoring, infrastructure management and so on.

The tremendous advantage of using information derived from remotely sensed data to correct, update, and maintain cartographic databases and geographic information systems (GE) has been amply demonstrated over the recent decades by studies and projects on various topics (Campbell, 1987). GIS and remote sensing have been developed as distinct spatial data handling technologies with their own methods of data representation and analysis for supporting vegetation analysis and modelling specifically (Goodchild, 1994). The advances in integration between GIS and remote sensing tool with development of computer software can provide powerful tool to acquire, store, retrieve, manipulate, analyze, and display these data according to user-defined specifications.

2.1.2 *Landsat-8 satellite*

Landsat-8 OLI/TIRS satellite was launched in February 2013, carrying the Operational Land Imager (OLI) and Thermal Infrared Sensor (TIRS) and has a 16-day repeat cycle over 185 kilometers swath (Irons, 2012). There are 9 reflective wavelength bands with 6 land application bands acquiring 30 meters resolution integrated inside the Landsat-8 OLI/TIRS satellite imagery (Irons, 2012). Landsat 8 was developed as a collaboration between NASA and the U.S. Geological Survey (USGS). NASA carried out the design, construction, launch,

and on-orbit calibration phases, during the period, the satellite was called the Landsat Data Continuity Mission (LDCM). USGS then took over routine operations and the satellite became Landsat-8. USGS oversees the post-launch calibration activities, satellite operations, data product generation, and data archiving at the Earth Resources Observation and Science (EROS) center.

Landsat-8 instruments obtain an evolutionary development in spatial technology. The operational land imager (OLI) improves on the previous Landsat sensors only acquired a technical approach represented by a sensor flown on other NASA owned satellite system. OLI is a push-broom sensor with a four-mirror telescope and 12-bit quantization. OLI collects data for visible, near infrared, and short wave infrared spectral bands as well as a panchromatic band. The new application provides two new spectral bands, one tailored especially for detecting cirrus clouds and the other for coastal zone observations.

Table 2.1. Specification of Landsat-8 OLI/TIRS

Landsat 8 OLI/TIRS		
Bands	Wavelength (μm)	Resolution (m)
Band 1—Coastal aerosol	0.435 - 0.451	30
Band 2—Blue	0.452 - 0.512	30
Band 3—Green	0.533 - 0.590	30
Band 4—Red	0.636 - 0.673	30
Band 5—Near infrared (NIR)	0.851 - 0.879	30
Band 6—Short-wave infrared (SWIR 1)	1.566 - 1.651	30
Band 7—Short-wave infrared (SWIR 2)	2.107 - 2.294	30
Band 8—Panchromatic	0.503 - 0.676	15
Band 9—Cirrus	1.363 - 1.384	30
Band 10—Thermal infrared (TIRS) 1	10.60 - 11.19	100 * (30)
Band 11—Thermal infrared (TIRS) 2	11.50 - 12.51	100(30)

2.1.3 Sentinel-2 MSI satellite

The Sentinel-2 satellites were launched in June 2015 having a 10-day repeat cycle over 290 kilometers swath and, is equipped with the Multi Spectral Instrument (MSI) which allows us to acquire 13 reflective wavelength spectral bands including 4 visible and near-

infrared bands with 10 meters resolution, 6 red edge, near infrared and short wave infrared bands with 20 meters resolution and 3 other bands with 60 meters resolution (M. Drusch, 2012). The Copernicus Sentinel-2 mission comprises a constellation of two polar-orbiting satellites placed in the same sun-synchronous orbit, phased at 180° to each other aiming at monitoring variability in land surface conditions. The main missions for the twin satellites system is to provide systematic global acquisitions of high-resolution, multispectral images corresponding to a high re-visit frequency and observation for the products of future operations, such as land-cover maps, land-change detection maps.

Table 2.2. Specification of Sentinel-2 MSI

Sentinel-2 MSI		
Bands	Wavelength (μm)	Resolution (m)
Band 1—Coastal aerosol	0.443	60
Band 2—Blue	0.492	10
Band 3—Green	0.559	10
Band 4—Red	0.664	10
Band 5—Vegetation Red Edge	0.704	20
Band 6—Vegetation Red Edge	0.74	20
Band 7—Vegetation Red Edge	0.782	20
Band 8—Near Infrared (NIR)	0.832	10
Band 8A—Vegetation Red Edge	0.864	20
Band 9 —Water Vapor	0.945	60
Band 10—Shortwave Infrared (SWIR) - Cirrus	1.373	60
Band 11—Shortwave Infrared (SWIR)	1.613	20
Band 12—Shortwave Infrared (SWIR)	2.202	20

2.2 Image classification

2.2.1 Pixel-based classification methods

For land use and land change (LULC) classification, pixel-based classification is considered as the traditional approach based on statistical analysis of individual pixels (L. Wang, 2004). This consideration for the approach of classification can be explained by the fact that the pixel is the fundam1ental (spatial) unit of a satellite image, and consequently it comes naturally and is often easy to implement .The procedures of pixel-based approach focus on spectral properties of individual pixels of the satellite images without considering any spatial

or contextual information of the study site (Robert C. Weih, 2010). In the ideal circumstances, pixel-based classification utilizes class characterizations which are defined and differentiated clearly which can sometimes be lacked in real life practice. In LULC studies, consistency and stability can be provided by classes, such as: water bodies, bare land, vegetation, but in details, problem can arise from various sources. The fundamental limitation that users of pixel-based method must face is the fact that surrounding pixels which may aid in identifying the target pixel are not utilized for classification. Normalized difference vegetation index (NDVI) and supervised maximum likelihood are some of the most common methods of pixel-based classification approach.

2.2.2 *Normalized difference vegetation index (NDVI) classification method*

Plants generally have low reflectance in the blue and red portion of the spectrum because of chlorophyll absorption, with a slightly higher reflectance in the green, so plants appear green to our eyes. Near infrared radiant energy is strongly reflected from the plant surface and the amount of this reflectance is determined by the properties of the leaf tissues: their cellular structure and the air-cell wall-protoplasm-chloroplast interfaces. These anatomical characteristics are affected by environmental factors such as soil moisture, nutrient status, soil salinity, and leaf stage (Machado, 2002). The contrast between vegetation and soil is at a maximum in the red and near infrared region. Therefore, spectral reflectance data can be utilized to calculate a range of vegetative indices that relate sufficiently with agronomic and biophysical plant parameters related to photosynthetic activity and plant productivity (Adamsen, 1999). The index is capable of predicting vegetation's photosynthetic activity as the vegetation index itself contains the near infrared and red light. With the vegetation pigment absorption, the compelling spectral relationship between the red and near-infrared red with the use of two or more bands can boost the vegetation signal which provide useful information (M. I. El-Gammal, 2014). Vegetation indices can provide a sufficient measurement to vegetation activity (Brown, Pinzon, & C.J., 2006). With the development of technology, most modern satellites are equipped with red and near infrared (NIR) making the application of NDVI more convenient and common in studies and researches of the recent decades. The NDVI is calculated from reflectance measurements in the red and near infrared (NIR) portion of the spectrum:

$$NDVI = \frac{(NIR\ Band - Red\ Band)}{(NIR\ Band + Red\ Band)}$$

2.2.3 *Supervised maximum likelihood classification method*

Maximum likelihood classification or supervised classification has shown its superior yield to unsupervised classification when training sites are appropriately provided with its powerful decision rule (Md. Mijanur Rahman, 2013). The classification method is often used for quantitative analysis of remote sensing data. The classification method requires users of supervised classification to supervise the pixel classification process. The various pixels values or spectral signatures that should be associated with each class must be specified by human control. The process includes the selection of representative sample sites of a known cover type called training sites. The computer determines the spectral signature of the pixels within each training area, and uses this information to define the statistics, including the mean and variance of each of the classes (Xavier Ceamanos, 2017). Accuracy of classification is highly dependent on the training sites selection which are required to represent the full range of variability within the class (Md. Mijanur Rahman, 2013). The computer algorithm then uses the spectral signatures from these training areas to classify the whole image. Ideally, the classes should not overlap or should only minimally overlap with other classes.

The maximum likelihood classifier is one of the most popular methods of supervised classification in remote sensing, in which a pixel with the maximum likelihood is classified into the corresponding class. The method is cooperated with the prior information and prior probabilities which is the occurrence of classes which are based on knowledge relating to classified area (H.Strahler, 1980). The performance of supervised maximum likelihood classification method rules out the inappropriate possibilities for particular pixels, thus, improve the classification accuracy.

2.2.4 *Object-based classification (OBC) method*

With the development of spatial technology, spatial resolution of satellite products are, as well, increasing overtime which provided an advanced approach as object-based classification focusing on as texture, tone and geometric features of objects (Qiong Hu, 2013) (Shao, 2012) (Yu Q., 2006). The approach was developed on the previous segmentation, edge-detection, feature extraction and classification concepts that have been used in remote sensing image analysis for decades (R. Kettig, 1976). However, OBC applications focusing on the identification and classification of target object's features which are increased in the amount of spatial information in one meter or less resolution imagery

strains the resources of image classification using traditional supervised and unsupervised spectral classification algorithms (G.J. Hay, 2008). The object-based term is broad and varies among different objectives; however; no matter how the method is applied, OBC must be based on the foundation of image segmentation. These segments are regions which are generated by one or more criteria of homogeneity providing additional spatial information compared to the traditional single pixel approach. The latest phase of OBIA research is directed more towards the automation of image processing which will provide a time efficient tool for natural resources monitoring particularly. With various advantages, the usage of OBC in monitoring of various purposes has been increasing in the recent years by scientific researches and studies reported by literature but has not been proven quantitatively (T.Blaschke, 2010).

2.3 Overview of mangrove

Mangroves are the group of various predominantly tropical trees and shrubs species at the intertidal zone that often face the harsh and dynamic natural condition (J.E. Sterling, 2006). Coastal mangroves can be found within the tropics and subtropics between approximately 308 N and 308 S latitude (Long, 2014). The term 'mangrove' is used to describe the ecosystem and the plant families that have developed with distinguished adaptations to survive at the coastal environment (Tomlinson, 1986).

With the typical habitat, they develop in various environmental conditions and possess unique adaptive characteristics such as salt-excreting leaves, exposed breathing root system, and productive viviparous propagules (Duke, 1992). Mangrove forests are found as separated group of dwarf stunted trees – in given high salinity and/or disturbed natural conditions while in more favored estuaries condition, mangroves can extend to kilometers to terrestrial area (FAO, 2007).

Mangroves have been widely used and exploited throughout the history in coastal countries around the world with precious values for various purposes. The knowledge about their current and past extent, condition and uses are valuable for forest managers and decisions makers. The ecosystem of mangroves provides various important functions and services at the level of local and national. The rural population not only relies heavily on the wood resources and non-wood resources from mangrove forest area but is only protected from harsh natural conditions and disasters with the natural fences created by the expanding mangroves area along the coasts. Moreover, the conservation of biological diversity is supported by the mangrove forest with natural habitat, nutrients, nurseries and so on.

The exact number of total mangrove species are still under discussion; however; it can be classified into a few plant families, such as Rhizophoraceae, Avicenniaceae and Combretaceae family that have e developed physiological and structural adaptations to the brackish water habitat. Although the scientists around the world have provided various and extensive studies on mangrove forests focusing on cases presenting mangroves' dynamic over different temporal and spatial scale, comprehensive information on the status and trends in the extent of mangroves has been lacking.

2.3.1 Mangrove status in the world

The estimations of global mangrove forest area vary among different projects and reports. In the first effort to estimate the total mangroves area worldwide, study conducted by Food and Agriculture Organization (FAO) and United Nations Environmental Program (UNEP) reported approximately 15.6 million ha of mangrove forest being detected in 1980 while more recent studies' estimations range from 12 to 20 million ha (FAO, 2007).

The largest area of mangrove forest occurred in Asia with 42%, followed by Africa with 20%. The proportion was 15% in North and Central America, 12% in Oceania and 15% in South America (Thomas N, 2017). The estimated total number of mangrove species distributing worldwide varied from 50 to 70 different species in which Asia found the highest species diversity despite its low forest cover in term of percentage of land area. Coastal mangrove forests often face great pressure from human activities with different land use type creating competition for agriculture, aquaculture and tourism indicating an alarming loss of the forest area. It was reported that Asia lose the most area of mangrove forest by 1.9 million ha since 1980.

However, the rate of mangrove lost globally has decreased down to approximately 0.5% per year in the recent years (FAO, 2007) with the conversing efforts from various environmental organizations and projects. Plantation and natural regeneration programs have been long implemented in many countries to help increase the mangrove forests' extent sustainably.

2.3.2 Mangrove status in Vietnam

There are 29 different provinces and cities that have the distribution of mangroves and their typical coastal wetland habitat. These cities and provinces are mostly located in the coastal area of the North, South East and South West of Vietnam. The total area of mangrove of Vietnam in 1943 was more than 250,000 ha; however; the number took a rapid fall to approximately 168,689 ha reported in 2014. The mangrove forests soar in the Mekong delta

area with most of the South West provinces and cities contributing almost 70% of the total mangrove forest area of Vietnam. It is estimated that the mangrove forest areas in South West of Vietnam is the largest with 89,837 ha, followed by the South East with about 42,000 ha and 20,486 ha in North East. Plant composition, distribution and development of mangroves particularly in Vietnam are heavily influenced by salinity level, climate condition, tidal regime and site condition (Phan Nguyen Hong T. V., 1999) in which, tidal regime is the vital factor that affect greatly to mangrove forest structure. Some of the main mangrove species distributing in Vietnam are Rhizophora apiculate *Rhizophora mucronate*, *Bruguiera gymnorrhiza, Avicennia alba, Avicennia marina, Sonneratia alba and Nypa fruticans.* The mangrove ecosystem has been damaged significantly by both human activities. The loss of forest can be closely linked with mangrove resources exploitation, land use change for agriculture, tourism, etc. resulted from the pressure from economic development and increasing population in the recent decades. Land degradation, water pollution, spreading plant diseases, abandoned bare land, erosion and high salinity level at coastal areas are the clear consequences that government has to the face when trying to conserve the valuable mangroves area.

2.3.3   *Remote sensing application on mangrove forest management*

Understanding the various advantages of mangrove forests and the emerging problem of increasing mangrove area loss, efforts are being made to provide better management and conservation of the coastal forest extent at national scale. The comprehensive and timely requirement of data used for decision-making and management of the mangrove forests makes the conventional method of collecting data become more challenging to provide large scale collection of information of an entire country. On the other hand, the synoptic, repetitive and multi-spectral features of remote sensing technology make it suitable to meet the requirement for an exclusive assessment of such dynamic characteristics of mangrove forest through time and space (Bahuguna, 2001). The importance of remote sensing data in mapping, monitoring and planning of forests in general and mangrove forests in particular, has been well-established. Various components of the coastal ecosystem are informed by the satellites, such as: wetland condition, coastal land form, shoreline changes, brackish water area, suspended sediment dynamic, mangroves condition and density etc. proving its compatibility and powerfulness in spatial and temporal analysis (F. Blasco, 1998).

For decades, remotely sensed data has been used to acquire information and data on the condition and extent of mangrove forests with various satellite materials, from low to very high spatial resolution imagery, and many different classification approaches in order to find out the most effective solution for threatened mangrove ecosystems (Wang, Sousa, Gong, & Biging, 2004) (Spalding, 1997) (Vaiphasa C. O., 2005). Although it is essential to note that no universal choice of classification method and satellite data have been given for mapping mangrove forest (Congalton, 2001) (Hankui K. Zhanga, 2018) (Heumann B. W., 2011), the major focuses are primarily corresponded with new, more or less complex and specific algorithm, applied to satellite data processing which combines the computation of various indices and classic method such as NDVI, maximum likelihood, minimum-distance classification (Bahuguna, 2001). Examples of pixel-based approaches have provided the discrimination possibilities for mangrove vegetation from neighboring LULC type. However, later studies also showed that the exploitation of multi-spectral advantages of pixel-based classification methods produced moderate poor results (Neukermans, 2008) (Vaiphasa C. S., 2006), object-based approach was proposed with the purpose to make use of more spatial information than pixel-based approach.

The availability of commercial satellite for several decades is extremely useful for mangrove forest monitoring; however; high spatial resolution imagery products can cost thousands of dollars for several kilometers squared scene creating great financial challenge for most researches and studies. The usage of medium-resolution is another solution that also provide multispectral surface data on desired scales which can be freely accessed by users with different purposes. Although high spatial resolution, such as IKONOS or QuickBird can open much more possibilities of improving discrimination among mangrove and other vegetation covers, less superior imagery products, such as Landsat-8 and Sentinel-2 has proven its effectiveness in mapping mangrove forest at regional scale, especially with mangrove and non-mangrove cover classification in number of studies (Aschbacher, 1995) (Rasolofoharinoro, 1998) (Selvam, 2003) (Gao, 1998) (Brown, Pinzon, & C.J., 2006) (Hankui K. Zhanga, 2018).

Intensive field campaign is essential for a highly accurate differentiate of mangroves and other neighboring land cover (Claudia Kuenzer, 2011). Profound understanding of the local knowledge and field work activities are required to calibrate and verify classification result. However, mangrove ecosystems are often inaccessible or complex making field work more challenging.

Overall, remote sensing technology have been applied for the management of mangrove forests for decades for its advances in spatial and temporal meaning. Studies involving mapping and classifying different LULC have suggested various promising classification approaches and satellite materials at multiple scales. The availability of freely-accessed satellites' imagery, such as: Landsat-8 and Sentinel-2 was mentioned as a great advantage in monitoring mangrove forest at different scales and delineating the dynamics of mangrove forest extents through time. However, studies about the application of remote sensing on mangrove forest in Ninh Binh province are very limited, thus, this study aims to delineate the usage of free access satellite materials to discriminate mangrove forest cover in the province.

CHAPTER 3 : GOAL, OBJECTIVES AND SCOPE

3.1 Goal

Providing scientific basis for remote sensing application for better management of mangrove forest in Ninh Binh province.

3.2 Objectives

Steps need to be taken in order to accomplish the study's goal. Specific objectives are clarified to illustrate the steps to provide scientific basis for mangrove forest in Ninh Binh province with the remote sensing application. Specific objects are stated as following:

- Constructing thematic map of current mangrove forest in Ninh Binh province and estimating the mangrove forest extent area.
- Assessing and comparing the classification accuracy of pixel-based and object-based approaches with Landsat-8 and Sentinel-2 satellite images.
- Constructing dynamic map of mangrove forest in Ninh Binh province within the period of 2013 to 2019 using multi-temporal remote sensing data.
- Quantifying the changes of mangrove forest extent in Ninh Binh province from 2013 to 2019.
- Proposing appropriate remote sensing approaches and further study for the mapping of mangrove forest area in Ninh Binh.

3.3 Study scope

Ninh Binh province is located in northern Vietnam with the population of 169,000 and total area of 215 km^2. The province is bordered by four provinces, including: Thanh Hoa province, Ha Nam province, Nam Dinh province and Hoa Binh province. These provinces were separated from Ninh Binh province by natural barriers. Tam Diep mountain range spreads from the North West to South East direction of Vietnam differentiating Ninh Binh province to Thanh Hoa province. Day river separates Ninh Binh province from Nam Dinh and Ha Nam province. The economic structure of the province focuses mostly on the industrial and service sector with the annual average GDP growth of 15.35% per year (Cuc, 2011).

There are two main rivers running through the province, the Red River and the Ma River. The climate is tropical monsoon with hot season from April to October and cold season from November to March. Recorded average annual temperature stays at 24°C and the average

annual rainfall is 1760 mm (Nguyen Khanh Van, 2000). The tidal cycle in the region ranges within 23 hours with the mean tidal amplitude varying from 150 to 180 cm with the high tidal inundation during the cold season from December to February (Phan Nguyen Hong V. T., 2004).

Comparing with other provinces within the Red river delta, Ninh Binh province has the largest forest area with the total area of more than 19,000 ha, including both natural and plantation forests. Mangroves are among different plantation forest types in Ninh Binh, especially along the coastal line where wetland habitat is common.

The topography of Ninh Binh is divided into three main types of terrains: Delta area, mountainous area and coastal area. The most populated area is located at the delta area with almost 90% of the population. Spanning over 100,000 ha, the delta area has the highest area percentage of more than 70% of the province with the main livelihood focus of agriculture. Mountainous area of Ninh Binh province is situated along the Tam Diep range with the total area of 35,000 ha up to 24% of the whole province including parts of 5 different districts. The smallest terrain is the coastal area with only 6000 ha stretching along 15 km of the country's seashore taking up 5 communes of Kim Son district in Ninh Binh province.

Current coastal land area is expanding beyond the official boundaries due to sediment accumulation in the whole Red River Delta. Cuc (2011) reports that the land expansion averages 28 meters per year for the whole Red River Delta. Boundary of the study site was based on data obtained during field visits and with the aid of Google Earth Pro software to eliminate unnecessary areas and to improve the image processing performance. The mangrove forest in Ninh Binh province is located mainly on the east coast within a relatively small area due to historical causes: the mangrove forest plantation project conducted by Japanese Red Cross (JRC) in the 1990s at the coastal zone of Kim Son district was limited to a certain area with clear zonation (International Federation of Red Cross, 2009) that remains until today as verified during field visits. The 15 km long coastal line of Ninh Binh province provides habitat for more than 500 different animal and plant species, including 50 species of both plantation and natural mangrove plant.

Specific study site for classification processing was determined corresponding with reference material from Google Earth Pro software. The mangrove forest area of Ninh Binh province is separated with the other mangrove forest areas of Nam Dinh and Thanh Hoa province by the rivers on both sides making a clear administrative boundary for the study site. Shape file of study site's boundary was created in Google Earth Pro software using "add polygon" tool which was later exported in KML. file format and converted to KMZ. format

by "conversion' tool in ArcMap 10.4 software. Thereafter, different classification methods were applied on the specified study site area to reduce redundant information that can affect the discrimination result between mangrove forest cover and other types of land cover.
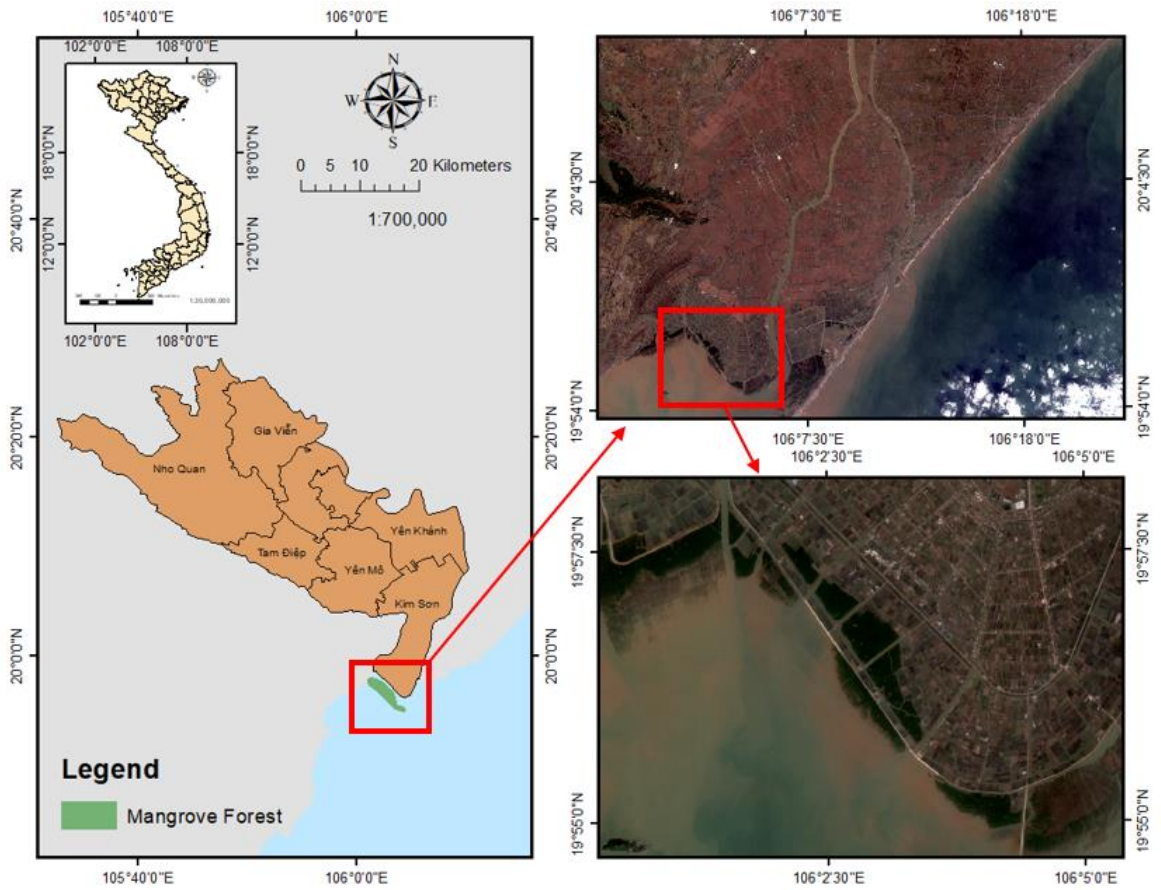
Figure 3.1. Study site map

a) Map of Vietnam and Ninh Binh province; b) Sentinel-2 image showing coastal area of Ninh Binh province; c) Sentinel-2 image showing study site at the coastal area of Ninh Binh province

CHAPTER 4 : METHODOLOGY

4.1 Materials

4.1.1 Satellite images selection

Most of mangrove forests habitat in the unique wetland areas which are periodically submerged by high tide at certain time; thus; the detection mapping results vary significantly by the contrasting signature for the forest which can result in underestimating mangrove forests area (Xuehong Zhanga, 2017). There are many techniques as well as technology can be applied to reduce the impact of tidal regime on mangrove forest mapping accuracy; however; most of the solutions are rather costly and require different sensor types in order to eliminate the sea-water submerging target forest area. Tidal characteristics of the Tonkin Gulf coast where the mangrove forest coastal area of Ninh Binh province located studies can be valuable references to determine the consistent mangrove forest boundary.

Neap tide and spring tide are stages of tide when the sea water level drops and rises significantly, especially at the coastal areas. The frequency of tidal inundation (hydroperiod) is the principal control on the distribution of mangrove communities (Kuenzer, 2011). Thus, it is difficult to develop an automated classification algorithm that works consistently across different tidal stage. According to Kerrylee Rogers (2017), the classification process should correspond with different tidal stage to enhance the consistent discrimination of the mangrove forest as his study showed a significant increase in overall accuracy when combining pixel layers of a classification method with satellite images taken in different dates which was believed to be at multiple tidal stages basing on automatic tidal estimation algorithm and tidal regime behavior studies.

Locating along the shoreline of Red River delta of, the tides of Ninh Binh province are diurnal with a neap tide–spring tide cycle of 14 to 16 days (Minh Luu, 2014). Online archives at https://earthexplorer.usgs.gov/ software of Sentinel-2 and Landsat-8 allow users to download previous satellite images at the calibration of 5 and 16 days respectively. By selectively accessing Sentinel-2 and Landsat-8 imagery from the archive, we were able to present spectral reflectance of mangrove at different tidal stages with cloud-free scene images with acquisition dates following the low and high tide cycle. Thus, we selected 4 images of each satellite with adjacent cloud-free scenes that were taken 14 to 16 days apart. Landsat-8 multi-temporal data were obtained for quantifying the changes of mangrove forest extents and constructing current thematic map of mangrove forest in Ninh Binh province.

The online archive at https://earthexplorer.usgs.gov/ provide long-term and free accessing collection of Landsat-8 and Sentinel-2 satellite imagery for the multi-temporal delineation of mangrove forest extents changes at Ninh Binh province. Images, from 2013 for Landsat-8 and from 2015 for Sentinel-2 due to launch time of the satellite aircraft, were selectively assessed and downloaded from the archive with cloud-free adjacent scene condition of the study site from the online archive.

Table 4.1. Details of remote satellite images selection

Image type	Product ID	Date of Acquisition
Landsat 8 OLI/TIRS	LC08_L1TP_126046_20131008_20170429_01_T1	08/08/2013
	LC08_L1TP_126046_20190603_20190618_01_T1	03/06/2019
	LC08_L1TP_126046_20190619_20190703_01_T1	19/06/2019
	LC08_L1TP_126046_20190705_20190719_01_T1	05/07/2019
	LC08_L1TP_126046_20190721_20190801_01_T1	21/07/2019
Sentinel-2 MSI	L1C_T48QXH_A010869_20190406T032806	06/04/2019
	L1C_T48QXH_A011055_20190419T033830	19/04/2019
	L1C_T48QXH_A020178_20190504T033029	04/05/2019
	L1C_T48QXH_A020464_20190524T032920	24/05/2019

4.2 Methodology

The methodology of this study encompasses the selection of satellite images, pre-processing for Landsat-8 images with Top of Atmosphere (TOA) correction, different classification methods, composition of pixels layers, assessing of classification accuracy, constructing mangrove dynamic map and quantifying the changes of mangrove extent within given period. The methodology is presented as flowchart in figure 5.1.
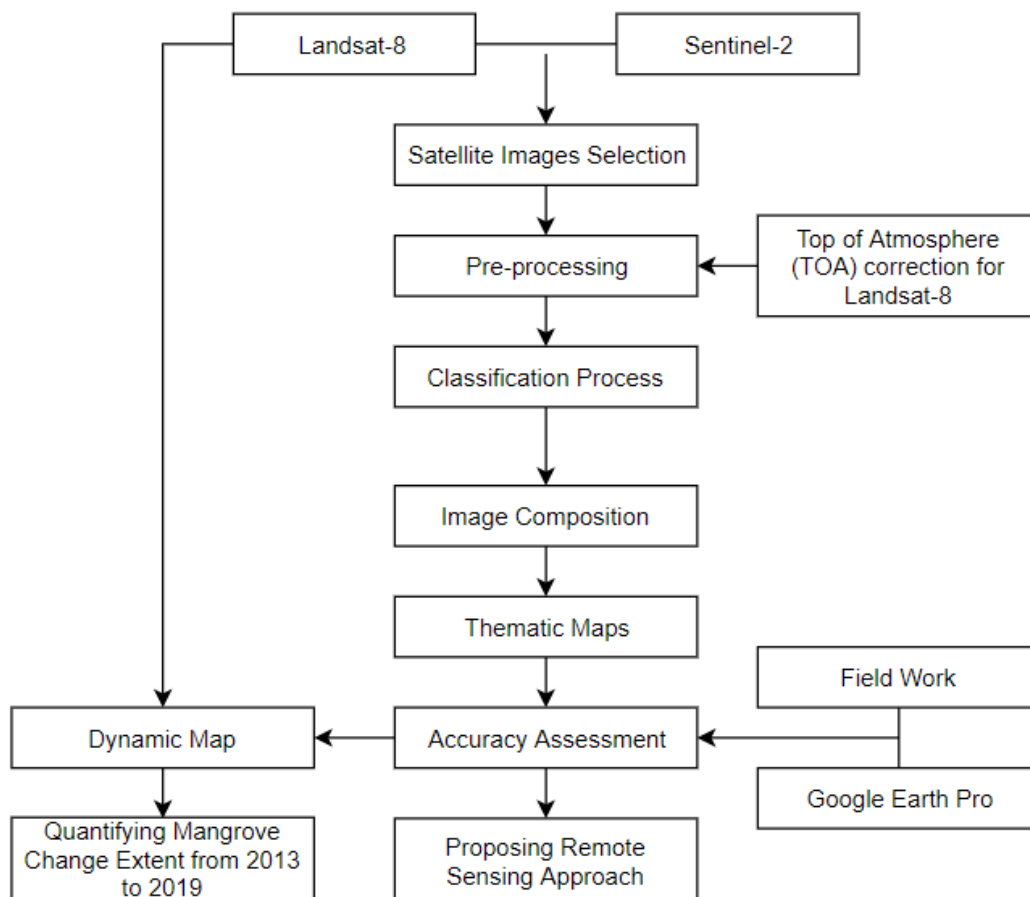
Figure 4.1. Flowchart of methodology

4.2.1 Field work

In March 2019, two field visits to the mangrove forest area of Ninh Binh province were conducted to collect data for accuracy assessment and visual inspection as well as local knowledge about tidal regime. Location data on land use and cover classes were collected by the Garmin 78s Global Positioning System (GPS) device.

Simple random sampling method was carried out to assess the NDVI , supervised maximum likelihood and OBC classification methods independently with a minimum of 50 samples per class determined for purposes of the study in order to ensure optimized classification estimation (Congalton, 2001). The total 100 sample points for 2 classes of mangrove and non-mangrove cover type for the three classification methods were created using "random sampling" tool on ArcMap 10.4 software.
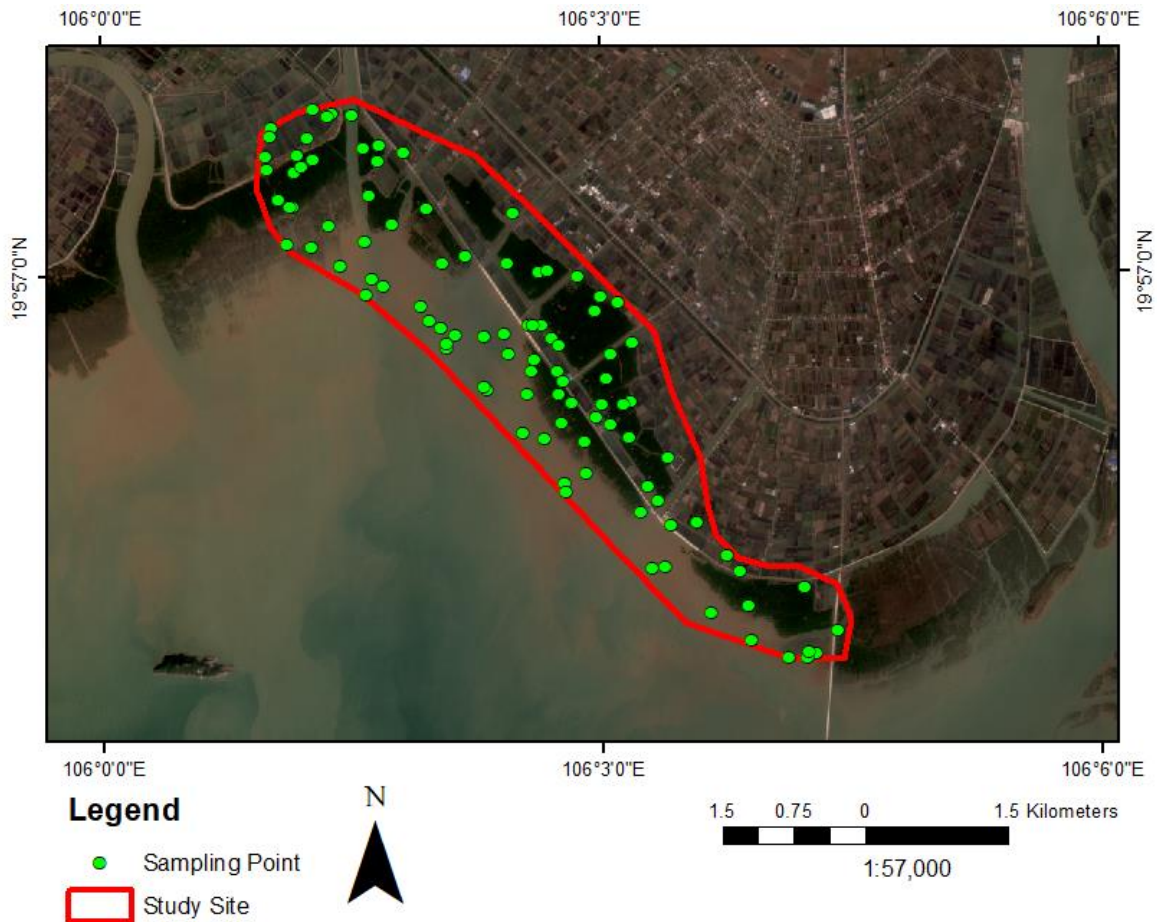
Figure 4.2. Sampling points for field data collection

4.2.2 Satellite images pre-processing

Landsat data are often required to preprocessed before analysis to reduce the changes in sensor, solar, atmospheric and topography impact on different image for desired specific purposes. The newly introduced Landsat 8 satellite is able to provide products processed with Operational Land Imager (OLI) and Thermal Infrared sensors (TIRS) (Young, 2017). In this study, we acquire the Landsat 8 OLI/TIRS Level-1 Collection 1 products which are processed at L1TP (Precision Terrain Level) level. The study required comparison among Landsat 8 satellite images among different time. Therefore, the digital number (DN) for necessary bands of Landsat 8 OLI/TIR for vegetation classification techniques were converted to top of atmosphere (TOA) with scaling factor and solar elevation derived from the given metadata of the products (Hankui K. Zhanga, 2018). The conversion was processed using the "Raster Calculator" tool in ArcMap software with the information given from metadata MTL file in the imagery product download from in accordance with the formula:

From Digital Number (NB) to top of atmosphere (TOA):

$$\rho\lambda' = M\rho Qcal + A\rho$$

20

Where $\rho\lambda'$ is the TOA reflectance value; $M\rho Qcal$ is the REFLECTANCE_MULT_BAND_x (x is the band number) and $A\rho$ is the REFLECTANCE_ADD_BAND_x (x is the band number) which can be found in the metadata file of Landsat 8 image.

Correcting Solar Angle:

$$\rho\lambda = \frac{\rho\lambda'}{\sin(\theta SE)}$$

Where $\rho\lambda$ is the TOA reflectance value after solar correction; $\rho\lambda'$ is the TOA reflectance value before solar correction and θSE is the solar zenith angle. Each of the band used for the study is converted to TOA and eventually, all of them are combined to a specific image with reflectance value assigned for each pixel

4.2.3   Satellite Image classification

4.2.3.1 Pixel-based classification method

Supervised maximum likelihood classification method:

Maximum likelihood classification was processed on ArcMap 10.4 software. The combination of band 2 ,3, 4, 5, 6, 7 was obtained from Landsat-8 data and band 2, 3, 4, 8, 11, 12 from Sentinel-2 data corresponding to red, blue and green band of the RBG band combination. In order to create the RGB band combination, the obtained bands of both satellites were composited on each other using the "Composite" tool in ArcMap 10.4 software.

It is essential that in order to maximize the classification accuracy, training sites for each class are determined carefully in comparison with Google Earth Images and other reference materials, such as: local people, previous map of the area, related documents, etc. with sufficient number, shape, varieties, homogeneities and distribution (Md. Mijanur Rahman, 2013). The training sites were created using "Draw polygon" tool and managed using "Training Sample Manager" tool. The results from training site process were reclassified into mangrove and non-mangrove cover class using "Reclassify" tool. Number of training sites, number of pixels selected, and total area of each class are summarized in Table 4.2 and Table 4.3.

Table 4.2. Training sites description of each class for Sentinel-2 images

Land Use/Land Cover class	Mangrove	Non-mangrove

No. of training site	45	37
No. of pixels	780	815
Total Area (Hectare)	7.80	8.15

Table 4.3. Training sites description of each class for Landsat-8 images

Land Use/Land Cover class	Mangrove	Non-mangrove
No. of training site	60	48
No. of pixels	937	558
Total Area (Hectare)	84.33	50.22

Finally, training sites assigned with given classes were automatically classified using "Maximum likelihood classification" tool to the final map and ready for accuracy assessment. The process of maximum likelihood classification is presented in the Figure 4.3.
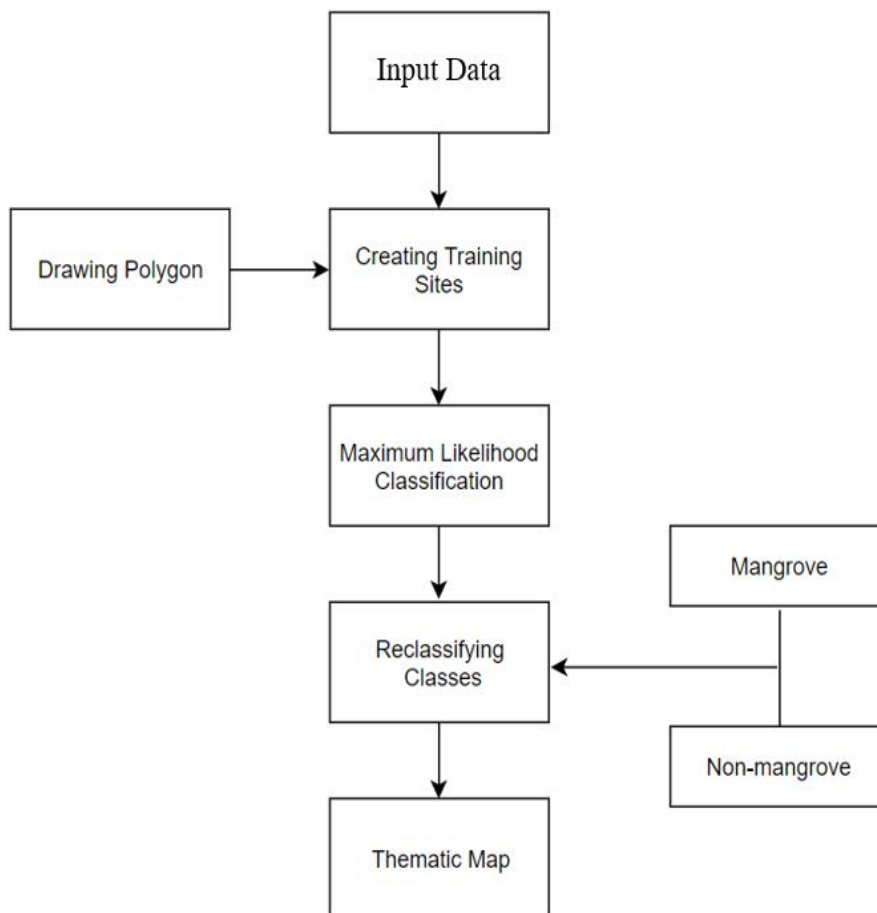
Figure 4.3. Flowchart of supervised maximum likelihood classification process

Normalized Difference Vegetation Index (NDVI) classification method:

The multi-spectral data of Landsat 8 OLI/TIRS and Sentinel-2 MSI can be utilized to enhance the detection of vegetation cover at the study area. The classification techniques acquire the red bands (R) and near-infrared (NIR) bands from both satellite images to emphasize on the density of plants (M. I. El-Gammal, 2004). For Sentinel-2, we obtained NIR-band 8 and R-band 4 while NIR band 5 and R band 4 were obtained from Landsat-8 which can be found in the metadata data set included from downloaded packages from https://earthexplorer.usgs.gov/ website. The classification was processed on ArcMap 10.4 software, the equation for the vegetation indices was calculated as following equation:

$$NDVI\ calculation\ of\ Sentinel-2\ images = \frac{(Band\ 8 - Band\ 4)}{(Band\ 8 + Band\ 4)}$$

$$NDVI\ calculation\ of\ Landsat-8\ images = \frac{(Band\ 5 - Band\ 4)}{(Band\ 5 + Band\ 4)}$$

The NDVI value ranges from -1 to 1 with values from 0.6 to 0.8 indicating temperate and tropical rain forests (Gross, 2005) where the recommended value range for healthy mangrove would be from 0.3 to 1 (Umroha, 2016). The characteristics of mangrove forest in Ninh Binh, however, often have lower height compared to typical mangrove forest of southern Vietnam. In addition, with many saplings and newly planted mangrove. According to visual inspection from high-resolution spatial reference from Google Earth Pro software, pixels were assigned with appropriate class according to their value calculated from the vegetation index formula using "Reclassify" tool.

Table 4.4. Recommended NDVI values for different LULC types

Classes	Description	NDVI value
Mangrove	- Dense and healthy mangrove area - Saplings and newly planted mangrove plants	0.1 – 0.8
Non-mangrove	- Bare land - Infrastructure - Grass land	-0.1 – 0.1

23

| | - Water | |
| | - Aqua-culture area | |

After the being reclassified into given classes, the results were ready for accuracy assessment. The process of NDVI classification method is presented at the flowchart in Figure 4.4.
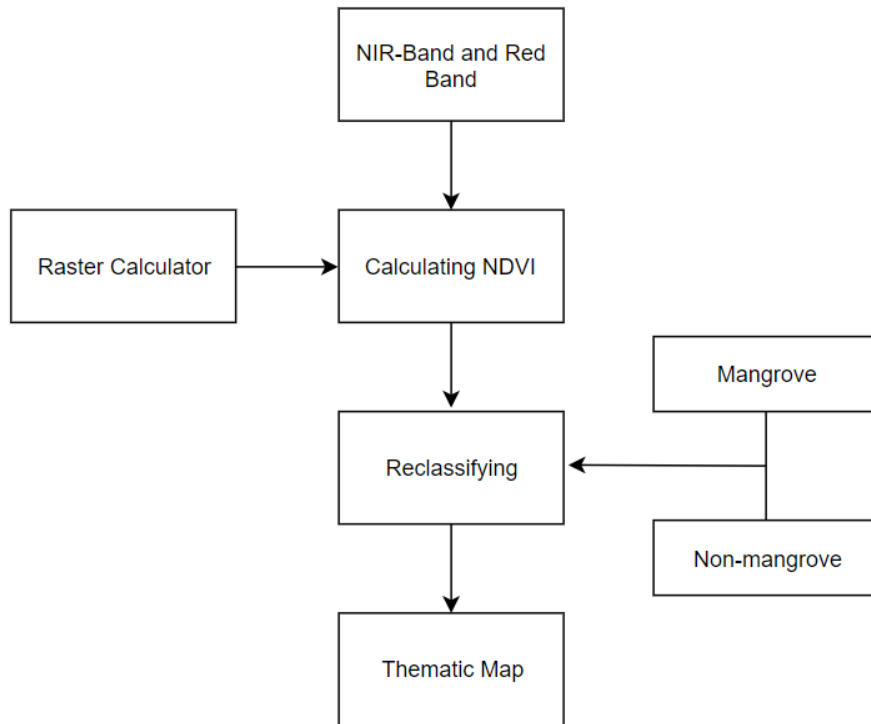
Figure 4.4. Flowchart of NDVI classification method process

4.2.3.2 Object-based classification (OBC) method

With the development of spatial technology, resolution of satellite products are, as well, increasing overtime which makes the pixel-based classification method restrain its performance in capturing the researcher's objectives as texture, tone and geometric features of objects cannot be utilized by the customary pixel-based techniques which results in statistical separability depletion among different classes (Qiong Hu, 2013) (Shao, 2012) (Yu Q., 2006). In this study, we took the advantages of the True Color Image (TCI) band combination of Landsat-8 and Sentinel-2 which were combined using the "Composite" tool in ArcMap 10.4 before being uploaded to E-Cognition Developer 9.0 software.

The Object-based image analysis was processed on the E-Cognition Developer 9.0, we followed the analysis process steps order as: multiresolution segmentation, selection of features or rules for classification, nearest neighborhood and classification.
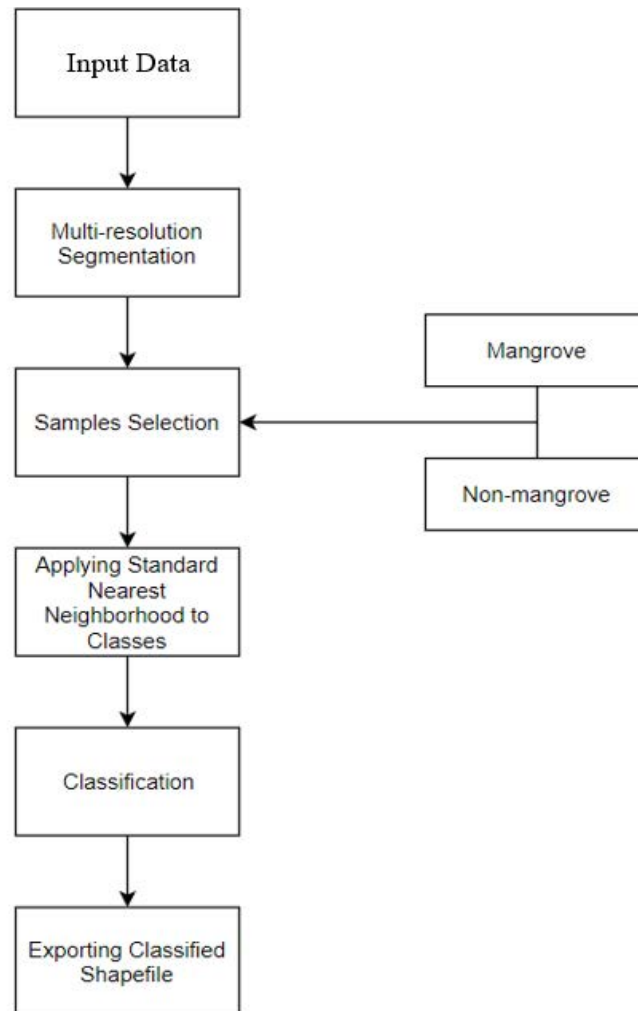
Figure 4.5. Flowchart of OBC classification

The appropriate configuration for the multiresolution segmentation process can only be acquired by trial-and-error approaches to improve classification accuracy. Segmentation configuration after being tested with different combinations of parameter and criterion were set as following.

Table 4.5. Parameters for segmentation configuration

Imagery	Scale	Shape	Compactness

Sentinel-2	30	0.3	90
Landsat-8	10	0.2	0.9

Training samples were selected carefully from the segmentation resulted from the multi-resolution process using "Select samples" tool. The selected samples were assigned into 2 classes of "mangrove" and "non-mangrove" class. The selection of training sites is presented at the table 4.6.

Table 4.6. Training sites description for "Select sample" tool

Satellite Imagery	No. of Training Sites	
	Mangrove	Non-mangrove
Sentinel-2	30	45
Landsat-8	20	31

"Nearest neighborhood" tool was used to classify the surrounding segmentations that had similar spatial patterns with sample ones of each class. Thereafter, the classified segmentation results of mangrove forest created in the E-Cognition Developer 8.0 software was converted into Shapefile format and clipped according to the study site by ArcMap 10.4 software.

4.2.4 Image overlaying

The classified layers of each satellite images were assigned with value 0 for non-mangrove class and value 1 for mangrove class. Preprocessing and classification methods were carried out on all images which were integrated with each other using the *"Raster Calculation"* tool of ArcMap 10.4 software. Image combination were created by overlaying 4 layers of classified pixels of the same satellite and classification method within the study site corresponding to different satellite image dates on top of each other. The result of "Raster calculation" tool provided 4 different values from value 0 for consistent non-mangrove class, value 1,2 and 3 for sub-merged mangrove class and value 4 for consistent mangrove class. The overlaying process was carried out on classification results of Sentinel-2 and Landsat-8 images. Mangrove pixels of the final map for accuracy assessment included consistent mangrove pixels that stayed above the water surface at all tidal stages and the submerged mangrove pixels which were inundated at one or more than one stages.

Thereafter, submerged mangrove and consistent mangrove were reclassified to mangrove class and consistent mangrove class was reclassified to non-mangrove class with "Reclassify" tool in ArcMap 10.4 software for the final map.

4.2.5 Assessment of image classification's accuracy

Simple random sampling method was carried out to assess the NDVI thresholds, supervised maximum likelihood and object-based image classification methods independently with a minimum of 50 samples per class determined for purposes of the study in order to ensure optimized classification estimation (Congalton, 2001). In this study, 100 sampling points were selected by simple random sampling method operated by the random sampling of ArcMap 10.4 software's tool corresponding with 2 classes of this study, as mangrove forests and non-mangrove. Google Earth Pro software was also used for visual inspection and zoning the sampling area. Coordinates of each sampling points were recorded in ArcMap 10.4 software and put into GPS devices to be located on the field. The task of the field work was to find out the class of the selected points by following the coordinates on GPS devices and filling fieldwork sheet.

After that, error matrixes were produced to report on the producer's accuracy, user's accuracy and Cohen's Kappa coefficient statistic for each classification method (Story M, 1986). The error matrix is presented as on the Table 4.7.

Table 4.7. Error matrix for accuracy assessment

Class	Mangrove	Non-mangrove	Reference Total	Accuracy (%)	
				Producer's	User's
Mangrove					
Non-mangrove					
Classified Total					

Overall Accuracy =   **Kappa statistic =**

4.2.6 Constructing dynamic mangrove forest map

Landsat-8 satellite images were selected for constructing dynamic mangrove map and quantifying changes of mangrove forest extent in Ninh Binh province. Comparing with Sentinel-2 satellite, Landsat-8's online archive started from 2013 as the Landsat satellite was launched 3 years earlier allowing user to access images from longer period, thus, a longer-term assessment can be achieved for almost 6 years. Thematic maps of Landsat-8 images in

2013 and 2019 constructed from classification process were obtained from the classification process to assess the changes occurred to mangrove forest at the study site. The highest accuracy assessed classification method was applied for constructing mangrove dynamic map. The two maps were compared with each other using overlaying algorithm in ArcMap 10.4 software. Before applying the algorithm, mangrove and non-mangrove classes were assigned as numerical value. The algorithm was processed by "Raster calculator" software, by adding assigned values together, changes within the period of 6 years were shown in the form of numerical values. The construction of dynamic map is presented at the flowchart in Figure 4.6.
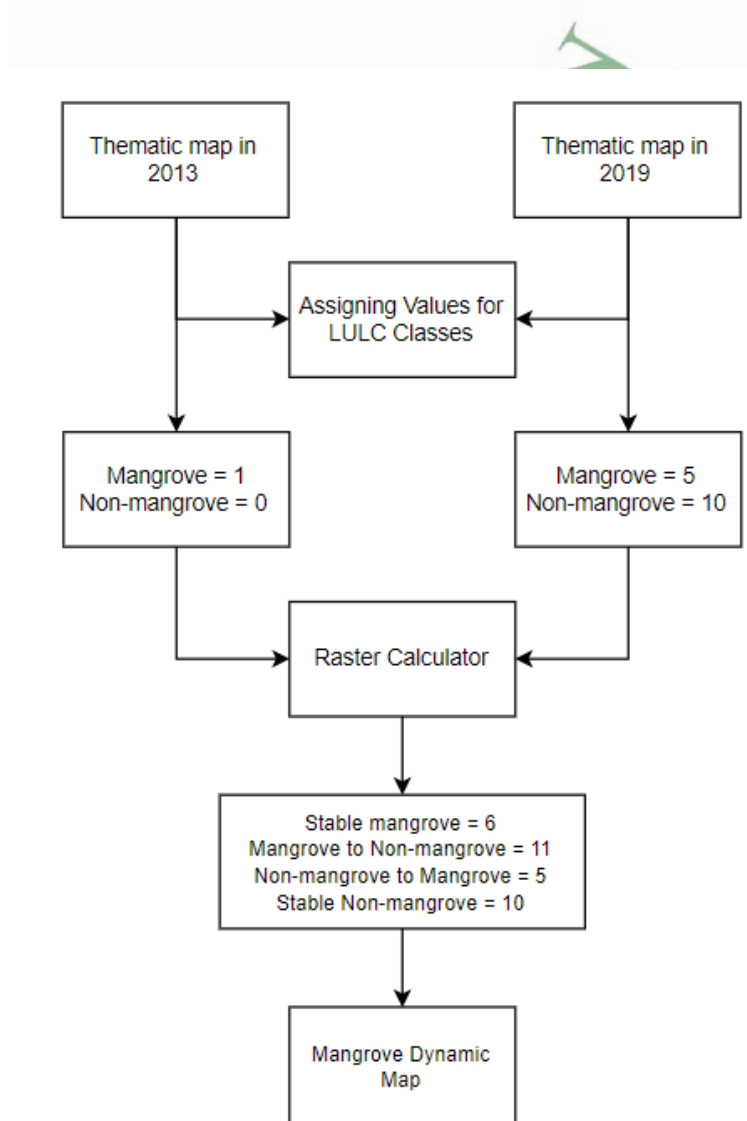
Figure 4.6. Flowchart of mangrove dynamic map construction

CHAPTER 5 : RESULTS AND DISCUSSIONS

5.1 Results

5.1.1 Image classification methods' results and thematic maps

The current status map of mangrove forest was constructed using Landsat-8 and Sentinel-2 satellite images with the application of three different classification methods: NDVI, supervised maximum likelihood classification and OBC. The usage of different satellite materials and classification approaches was able to detect a variety of mangrove forest area.

Table 5.1. Mangrove forest area detected by different classification on Landsat-8 and Sentinel-2

Satellite Image Type	Classification Method	Detected Mangrove Forest Area (Hectare)
Landsat-8 OLI/TIRS	NDVI	361.35
	Supervised Maximum Likelihood	331.11
	OBC	392.58
Sentinel-2 MSI	NDVI	378.56
	Supervised Maximum Likelihood	334.92
	OBC	322.53

Overall, the application of OBC method on Landsat-8 satellite image detected the largest area of mangrove forest with 392.58ha while OBC method on Sentinel-2 only showed 322.53ha. For NDVI, Landsat-8 and Sentinel detected 331.11ha and 334.92ha respectively. Finally, NDVI was able to classify 361ha with Landsat-8 and 378ha with Sentinel-2. Thematic maps of current mangrove forest extent are presented in Figure 5.3 to Figure 5.8.
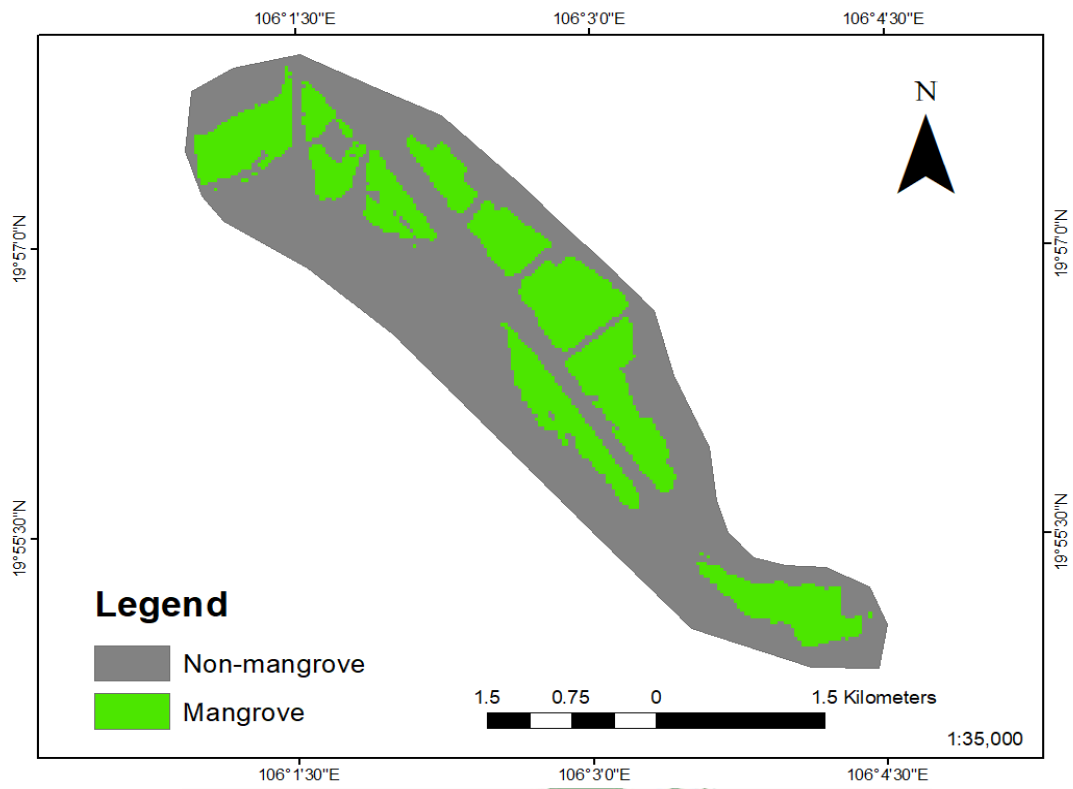
Figure 5.1. NDVI classification method with Landsat-8 images
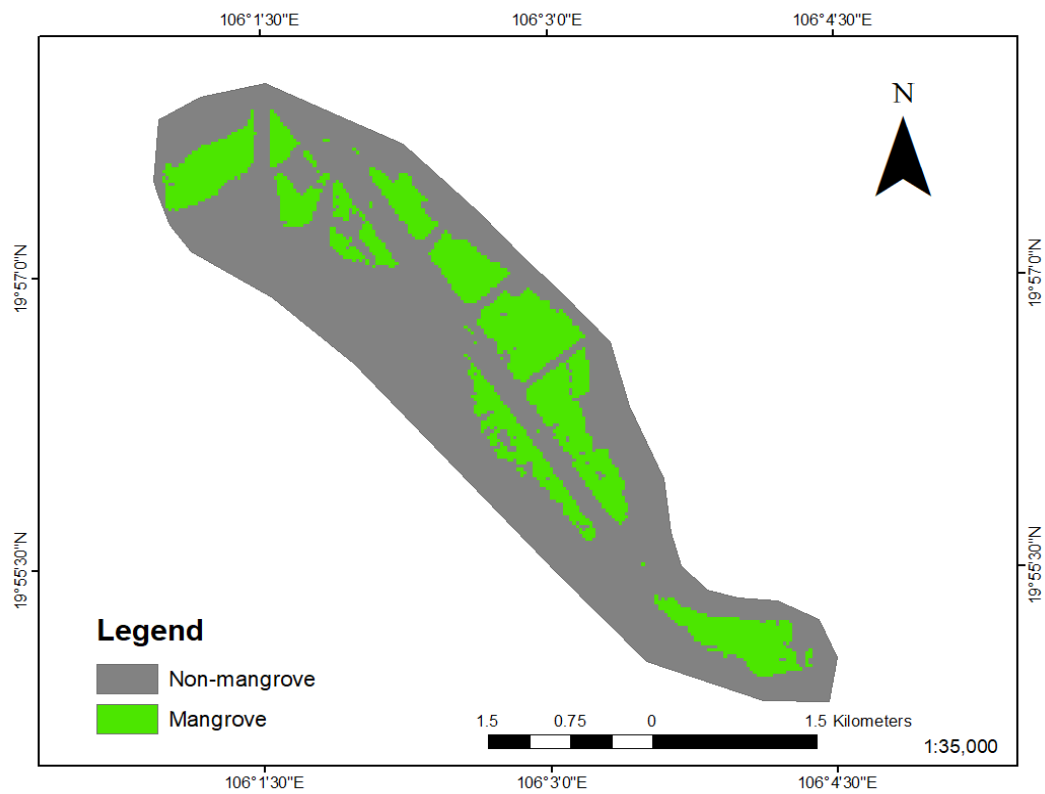
Figure 5.2. Supervised maximum likelihood classification method with Landsat-8 images
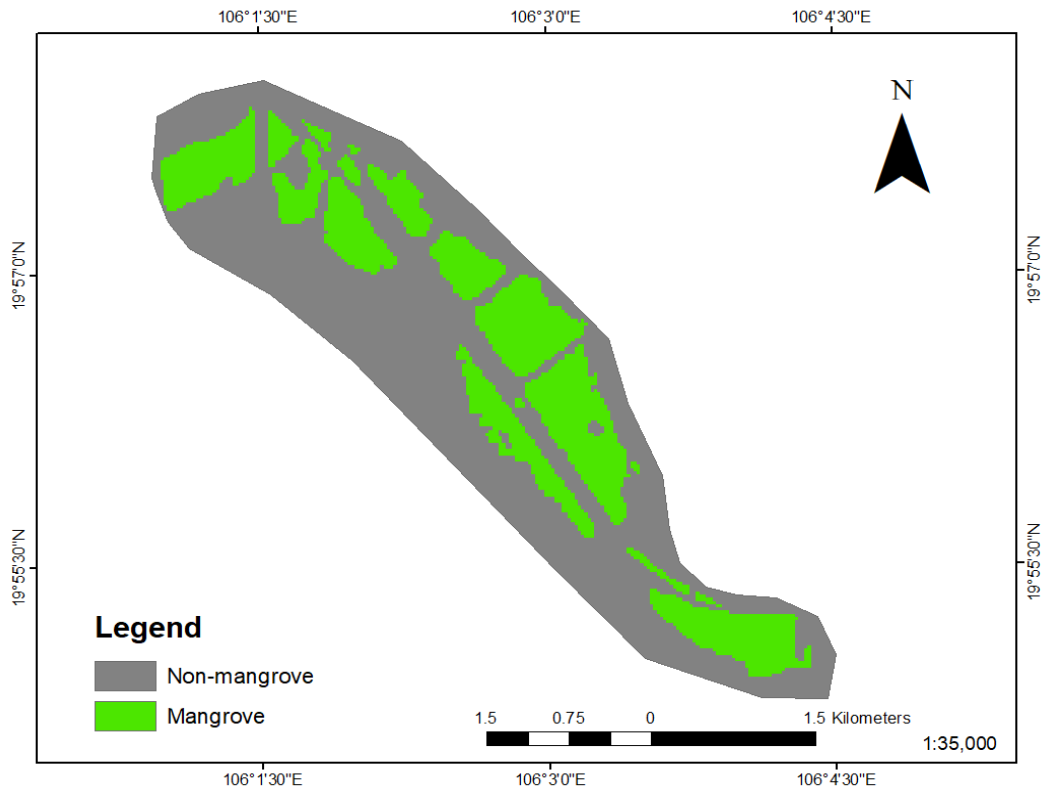
Figure 5.3. NDVI classification method with Sentinel-2 images
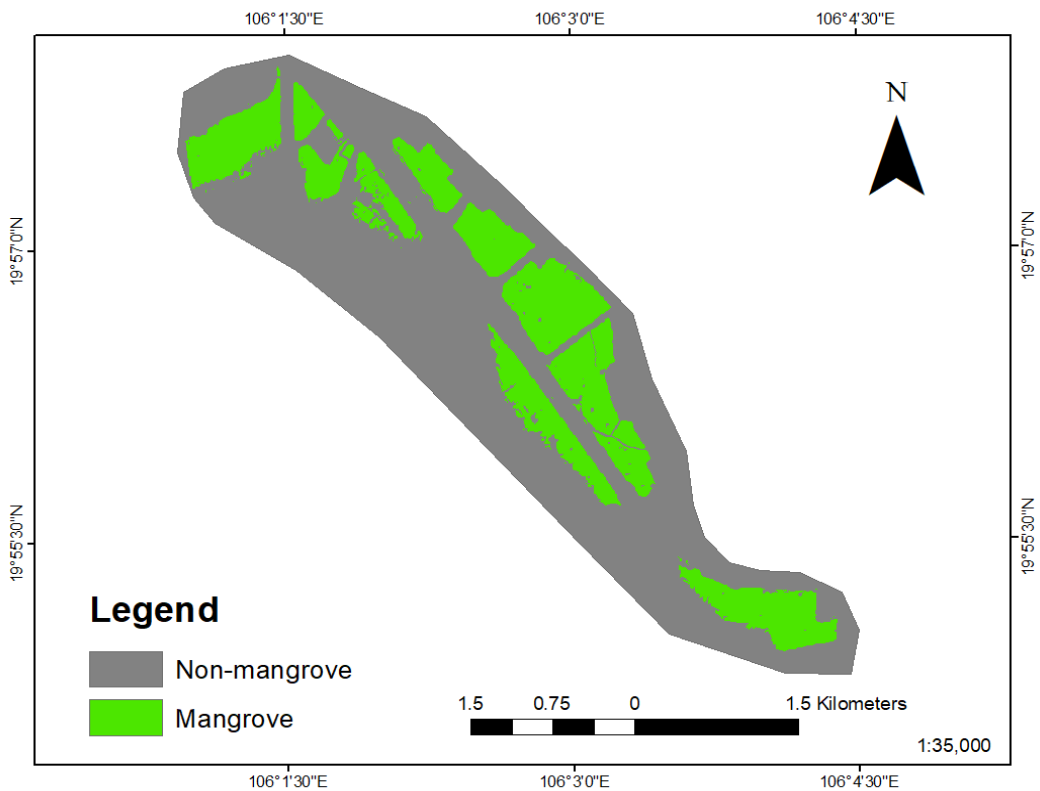
Figure 5.4. OBC with Landsat-8 images
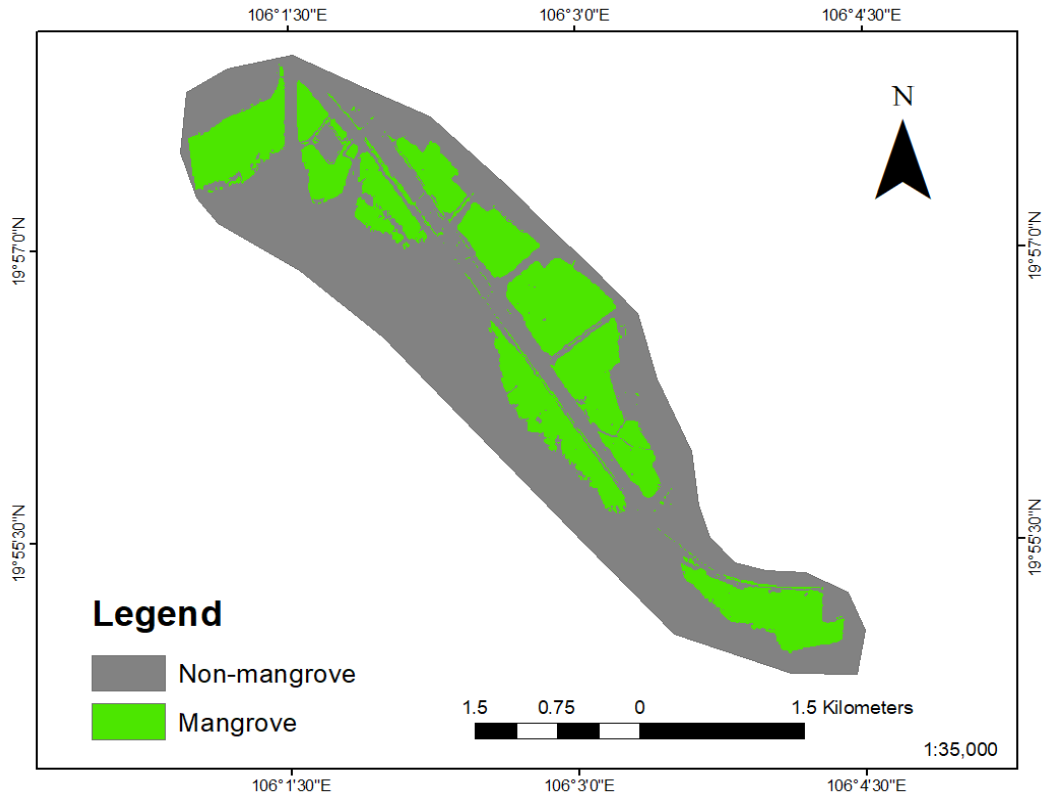
Figure 5.5. Supervised maximum likelihood classification method with Sentinel-2 images
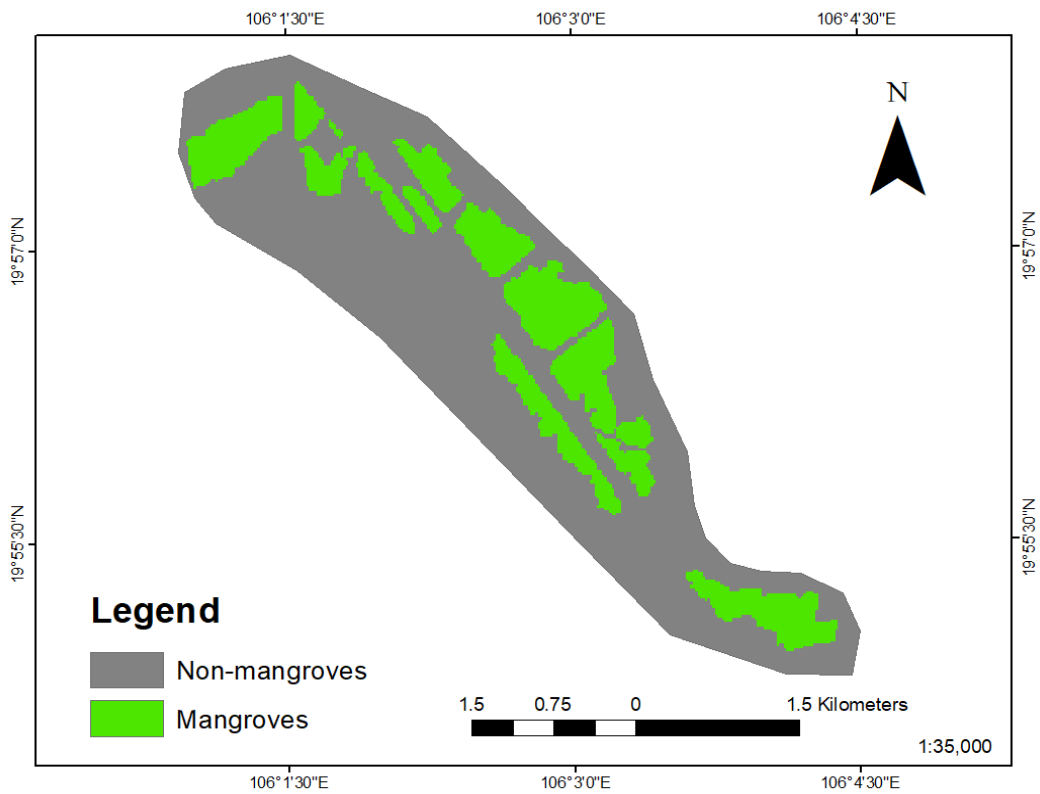
Figure 5.6. OBC method with Sentinel-2 images

5.1.2 Image classification methods' accuracy assessment

Results of the accuracy assessment based on simple random sampling method of all classification methods and satellite images are illustrated from Table 5.2 to Table 5.7. The accuracy assessment in this study included producer's and user's accuracy, overall accuracy and Cohen's Kappa coefficient statistic. Producer's and user's accuracy are used to determine the detection accuracy of each class while the Kappa coefficient measure the agreement for each class (Congalton, 2001).

Table 5.2. Error Matrix of NDVI classification with Landsat-8 images

NDVI classification method with Landsat-8				Accuracy (%)	
Class	Mangrove	Non-mangrove	Reference Total	Producer's	User's
Mangrove	50	11	61	94.34	81.97
Non-mangrove	3	36	39	76.60	92.30
Classified Total	53	47	100		

Overall Accuracy = 86%   Kappa statistic = 0.71

Table 5.3. Error matrix of supervised classification with Landsat-8 images

Supervised maximum likelihood classification method with Landsat-8				Accuracy (%)	
Class	Mangrove	Non-mangrove	Reference Total	Producer's	User's
Mangrove	47	14	61	94.0	77.05
Non-mangrove	3	36	39	72.0	92.30
Classified Total	50	50	100		

Overall Accuracy = 83%   Kappa statistic = 0.66

Table 5.4. Error matrix of OBC with Landsat-8 images

OBC method with Landsat-8				Accuracy (%)	
Class	Mangrove	Non-mangrove	Reference Total	Producer's	User's
Mangrove	52	9	61	85.25	85.25
Non-mangrove	9	30	39	76.92	76.92
Classified Total	61	39	100		

Overall Accuracy = 82%   Kappa statistic = 0.62

Table 5.5. Error matrix of NDVI classification with Sentinel-2 images

NDVI classification method with Sentinel-2				Accuracy (%)	
Class	Mangrove	Non-mangrove	Reference Total	Producer's	User's
Mangrove	53	8	61	91.38	86.89
Non-mangrove	5	34	39	80.95	87.18
Classified Total	58	42	100		

Overall Accuracy = 87%   Kappa statistic = 0.73

Table 5.6. Error matrix of supervised maximum likelihood with Sentinel-2 images

Supervised maximum likelihood with Sentinel-2				Accuracy (%)	
Class	Mangrove	Non-mangrove	Reference Total	Producer's	User's
Mangrove	49	12	61	94.23	80.33
Non-mangrove	3	36	39	75.0	92.30
Classified Total	52	48	100		

Overall Accuracy = 85%   Kappa statistic = 0.70

Table 5.7. Error matrix of OBC with Sentinel-2 images

OBC method with Sentinel-2	Accuracy (%)

Class	Mangrove	Non-mangrove	Reference Total	Producer's	User's
Mangrove	45	16	61	91.84	73.77
Non-mangrove	4	35	39	68.63	89.74
Classified Total	49	51	100		

Overall Accuracy = 80%   Kappa statistic = 0.60

The overall accuracy for Landsat-8 image were 86%, 83% and 82% with NDVI, supervised maximum likelihood and OBC method respectively while the percentages for Sentinel-2 were 87%, 85% and 80%. Overall, the thematic map constructed by NDVI classification method with Sentinel-2 satellite image achieved the highest overall accuracy with 87%.

Additionally, the Kappa statistics for Landsat-8 were 0.71, 0.66 and 0.62 with NDVI, supervised maximum likelihood and OBC method respectively while Sentinel achieved 0.73, 0.70 and 0.60 with similar classification method. Application of NDVI on Sentinel-2 image also gave the highest Kappa statistic with 0.73.

5.1.4 *Mangrove dynamic map and quantifying mangrove forest changes from 2013 to 2019*

Landsat-8 satellite images obtained from 2013 and 2019 were used for constructing mangrove dynamic map. The classification method used for assessing the changes within the period was chosen according to the accuracy assessment results as NDVI classification method with the overall accuracy of 86% comparing to other methods applied on Landsat-8. Thematic mangrove forest maps of 2013 and 2019 classified 2 main LULC of mangrove and non-mangrove. The changes of forest extent included the conversion of non-mangrove to mangrove cover, mangrove to non-mangrove cover and the stable area of mangrove forest and non-mangrove area.
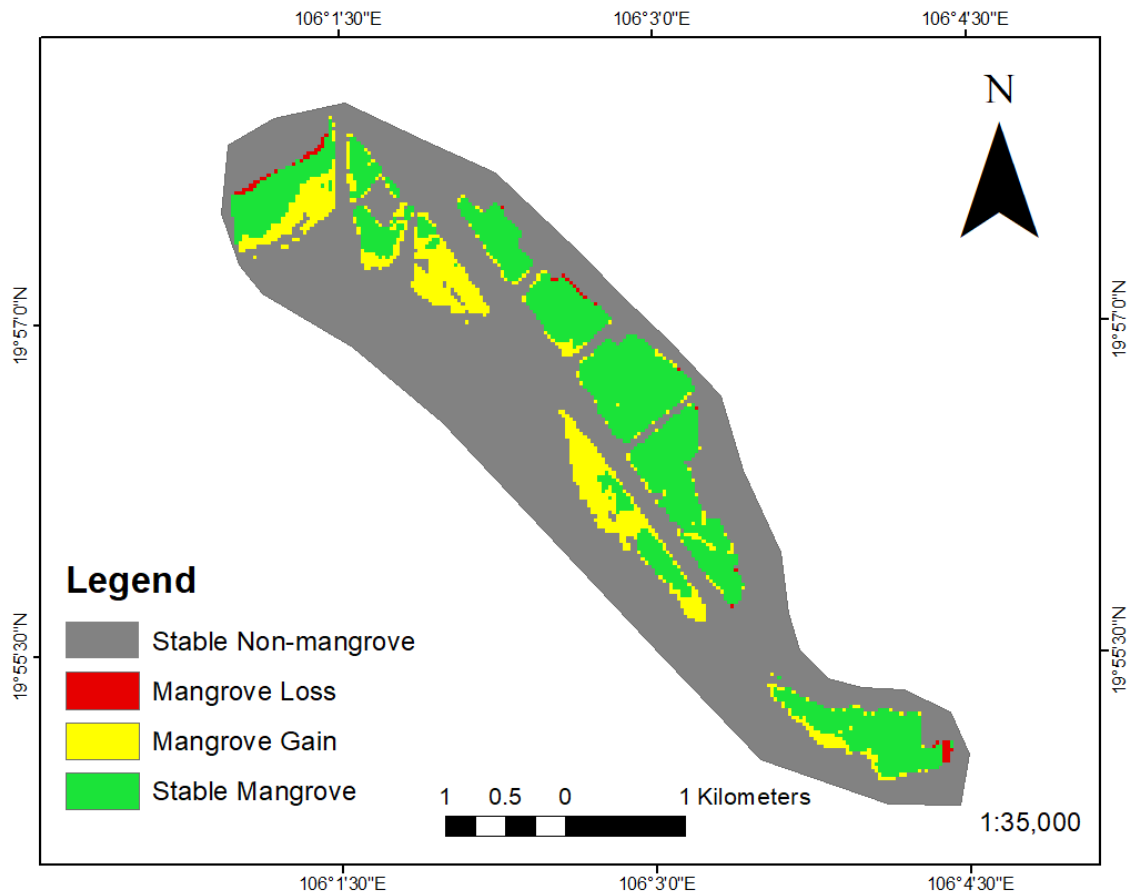
Figure 5.7. Mangrove dynamic map of Ninh Binh province from 2013 to 2019 using Landsat-8 images and NDVI classification

The dynamic map delineate four changes which occurred to mangrove and non-mangrove map in 6 years. The total area of mangrove forest detected by NDVI classification in 2013 was 262.08 ha while the area was 361.35 ha in 2019. Mangrove forest in Ninh Binh province experienced both mangrove loss and gain; however; the mangrove forest increased by almost 100 ha in total. It can be seen from the dynamic and field trip that, a large area of magrove was gained along the dike built along the coastal area of Kim Son province while small areas of less than 4 ha was loss at the fringe of densed planted mangrove zones. Most of the mangrove at the study site was results from different plantation projects conducted through out the years by organizations, such as: Japanese Red Cross (JRC), Ninh Binh Red Cross, Ministry of Natural Resources and Environment and so on. Since 2000, mangrove forest plantaion was developed fastly with the purpose of protecting coastal line, dikes and mitigating coastal soil erosion.

5.2 Discussion

5.2.1 *Suitable satellite image classification methods*

The classification method applied in this study can be categorized as a pixel-based classification, including NDVI and supervised maximum likelihood and an object-based classification, OBC. Both pixel-based and OBC methods represented by three specific methods adopted for this study often face the common problems of mixed zonation among forest areas, mis-classification of fringe and sparse mangrove when dealing with typical mangrove forests (Trang Nguyen, 2016).

NDVI and maximum likelihood supervised classification from the result showed considerable number of scattered pixels of the two classes mixing up together creating "salt and pepper" effect. Commonly, this effect is considered as a disadvantage of pixel-based classification method for mapping land use and land cover type (Yuehong Chen, 2018). However, correctly classified "salt and pepper" pixels increased the overall accuracy for classification of sparse distribution of mangroves. Boundary between mangrove class and non-mangrove class was difficult to be discriminated because fringe mangrove pixels were unclear and usually mixed with non-mangrove pixel.

In several previous studies, the application of image segmentation and specific-rules classification methods on OBC was not efficient in linking training sample areas with OBC of natural landscape because the visual interpretation can be rather vague comparing to human landscape (Heumann B. W., 2011) (Trang Nguyen, 2016) (Hu, 2013). OBC would likely to optimize the generalization or nearest neighborhood techniques to merge scatter pixels from "salt and pepper" effect into the surrounding pixels of other class as an effort to create coarser land use and land cover types. While clear zonation between mangrove forest class and non-mangrove class was achieved with OBC, mapping accuracy was reduced due to scatter misclassified pixels. Another factor to be considered was that common field sampling protocol is compatible with pixel-based classification as it does not focus on assessing the whole heterogeneous object, but single pixel reflectance leading to the field work becoming more time consuming for gathering OBC data (Heumann B. W., 2011). It is recommended that OBC requires further analysis in the field sampling as well as to set a rule of object classification to gain more spatial information. Although the multi-segmentation and class-specific rules application of OBC can provide more addition spatial pattern rather than just spectral information, the integration of low to medium spatial resolution remote sensing data with OBC can only achieved moderate accuracy when classifying mangrove class which has been recognized by studies of mangrove forest in similar coastal

environment in Vietnam (Ruiz-Luna, 1999) (Trang Nguyen, 2016) (Berlanga-Robles, 2002) (F. Blasco, 1998) (Horning, 2008).

Generally, with low to medium spatial resolution satellite imagery, such as: Landsat-8 and Sentinel-2, the application of pixel-based classification approach is widely suggested for mangrove forest mapping with high accuracy (Giri C. P., 2007) (Hernández Cornejo, 2005) (Giri C. K., 1996) (Béland, 2006) (Giri M. J., 2008). According to Seto and Fragkias (2007) in a systematic monitoring mangrove forest study in the Red river delta of Vietnam, they have successfully used the simple supervised classification and vegetation indices to map the area occupied by the mangrove forest extent using Landsat TM scenes. Other studies also showed successes when applying pixel-based classification approach in a similar environment, such as Aschbacher (1995), who assessed the mangrove forest structure and species composition in Thailand and Thu and Populus (2007) with their study on the current status and changes of mangrove forest in Tra Vinh province, Vietnam. However, there is also a great variation in image classification methods and algorithm. Investigations were carried out on the suitability of different classification methods to map extensive mangrove forest extents. According to literature, the application of supervised classification provides the most effective method for classifying mangroves based on medium spatial resolution imagery (Thu, 2007) (Aschbacher, 1995) (Giri M. J., 2008) (Heumann B. W., 2011) (Rasolofoharinoro, 1998). Supervised classification involves in transforming spectral information cooperating with different bands which improves the mapping accuracy overall.

However, this study, when comparing the accuracy of different classification methods, showed that NDVI classification method with Sentinel-2 image achieved the highest accuracy. This can be derived from the fact that supervised classification is often obtained for distinguishing mangrove cover from multiple other LULC types which may include not only infrastructures but also other vegetation types. Although NDVI only often shows use in pre-classification step for supervised or unsupervised, it shows high efficiency in differentiating between mangrove cover class and non-mangrove class which only include non-vegetation (Tong, 2004) (Thu, 2007) (Green, 1998). Strong correlation between NDVI data and mangrove canopy density for various satellite platforms was found in studies from Ramsey and Jensen (1996). The gap and closure in mangrove forest can provide valuable information on mangrove forest extent, health status and structure estimation. Not only can these inputs support the mapping of mangrove extent greatly but also contribute greatly to

the conservation and monitoring of mangrove forest by modeling of the ecological process including evapotranspiration, photosynthesis, primary production and so on.

Thus, the application of supervised classification can achieve higher accuracy in mapping mangrove forest in a more mixed environment, incorporating more LULC types of both vegetation and non-vegetation class. On the other hand, NDVI is more suitable for separating mangrove class from non-vegetation non-mangrove class, which is, in this case, for mapping mangrove forest extent in Ninh Binh province.

5.2.2 *Mitigating tidal regime impact on remote sensing processing*

In previous studies, the impact of tidal on classifications' results was often overlooked while combining images of multi-tidal stages were mostly undertaken to adjust the presence of cloud cover within scenes (Kerrylee Rogers, 2017) (Kirui, 2013). However, with the increasing interests in the mangrove ecosystem and spectral characteristics, the impact of tidal regime has been acknowledged more among studies about the application of remote sensing technology on mapping mangrove forest. The combinations of multiple tidal stages scenes can reduce the amount of pre-processing task for satellite images classification and improve its accuracy compared to single scene approach.

According to Kerrylee Rogers (2017) with his study on submerged mangrove forest area in Australia, it was shown that by exploiting the presence and absence of water in relatively low and high tide/neap and spring tide regime within the mangrove zones creating a multi-tidal combined image, the discriminability of mangrove zones will be improved along with the increasing accuracy of classification compared to standard approaches that only focus in classifying single mangrove scene.

Ideally, modelling the tidal regime activity requires a long term of recording field data and correlation estimation as variabilities are inevitable in predicting the tidal cycle. Several studies suggested that 30 years of tidal regime activity record from in situ stations would be sufficient to estimate the gap between neap and spring tide within a tidal cycle (Knudby, 2014) (Kovacs, 2001) (Kirui, 2013). However, such task is beyond the time and financial constraint of most researches (Kerrylee Rogers, 2017). In this study, due to the constraint of time and resources, studies on tidal regime of north coastal area of Vietnam and Ninh Binh province were obtained for the selection of satellite images used for multiple tidal scenes image overlaying. In further study, application of several software suggested by Kerrylee (2017) can be utilized to model tidal activity and put to use along with selection of remote

sensing data from satellites providing suitable calibration period. Moreover, acquisition of compatible remote sensing data that both fit in the given tidal cycle and cloud free adjacent scene condition can be challenging under the natural influence of weather. Thus, attempts to record actual tidal regime at different stages can also be conducted for long term period to improve the accuracy of classification and enhance the knowledge about mangrove ecosystem.

CHAPTER 6 : CONCLUSIONS

6.1 General conclusion

In this study, freely-available satellite images, Landsat-8 and Sentinel-2 were obtained for constructing current mangrove forest extent map and dynamic mangrove map as well as quantifying the changes of mangrove extent within the period of 2013 to 2018 in Ninh Binh province. Pixel-based classification approaches, including NDVI, maximum likelihood supervised, and OBC classification approach were tested on both satellites for classification accuracy. Selection of satellite images dates corresponding with tidal cycle from previous studies and image overlaying technique was obtained as an attempt to reveal the submerged area of mangrove and improve the discrimination result. The processing of satellite images on computer and field works has shown the results as following:

- The overall accuracy for Landsat-8 image were 86%, 83% and 82% with NDVI, supervised maximum likelihood and OBC method respectively while the percentages for Sentinel-2 were 87%, 85% and 80%. Overall, the thematic map constructed by NDVI classification method with Sentinel-2 satellite image achieved the highest overall accuracy with 87%. Additionally, the Kappa statistics for Landsat-8 were 0.71, 0.66 and 0.62 with NDVI, supervised maximum likelihood and OBC method respectively while Sentinel achieved 0.73, 0.70 and 0.60 with similar classification method.

- Along with previous studies, this study also suggested that the application of pixel-based generally produced higher accuracy, especially NDVI in detecting mangrove forest in Ninh Binh province, and the most accurate selection of satellite image and classification method was the using NVDI on Sentinel-2 MSI. The classification of Sentinel-2 MSI imagery data was able to detect 378.56 hectares of mangrove forest with an overall accuracy of 87%, producer's accuracy of 91.38% and user's accuracy of 86.89% corresponding with 0.73 level of Cohen's Kappa statistics.

- Landsat-8 images and NDVI classification method were used for constructing mangrove dynamic map and quantifying the changes of mangrove extent within the period of 2013 to 2019. Within the 6 years period, the mangrove forest area in Ninh Binh province increased by almost 100 ha compared to 262.08 ha in 2013.

6.2 Recommendation for further study and limitation

Although the study has provided valuable information for the scientific basis of remote sensing application on mangrove forest in Ninh Binh province, there were several limitations and challenges that have occurred during the research.

Due to the lack of stations recording tidal regime at the coastal line of Kim Son district, the study was soly based on theory from reference studies and secondary data from previous researches conducted at the study site. In situ data on coastal sea water level simutaneously with remote sensing data's acquisition time and field work would be valuable for modelling tidal activitiy using hydrology related software for a better image overlaying results. The superiority of multi-tidal stages compostion scenes was not significant as it could only achieved higher overall accuracy of 1% to 3% more than single scene approach. Moreover, OBC approach only produce moderate classification accuracy compared with others as it is suggested to be more compatible with higher spatial resolution remote sensing data integrated with field work guideline that is more compatible for OBC than pixel-based classification.

Further reseaches can look into the the integration of tidal study with acquisition of more field data relating to the current and historical tidal regime. The application of object-based can be improved with more pround and compatible field work guidelines.

REFERENCES

1. Adamsen, F. P. (1999). Measuring wheat senescence with a digital camera. *Crop sci*, 39: 719-724.

2. Aschbacher, J. O. (1995). An integrated comparative approach to mangrove vegetation mapping using advanced remote sensing and GIS technologies: Preliminary results. *Hydrologica*, 295, 285-295.

3. Aschbacher, J. O. (1995). An integrated comparative approach to mangrove vegetation mapping using advanced remote sensing and GIS technologies: Preliminary results. *Hydrologica*, 295, 285-295.

4. Bahuguna, S. a. (2001). Application of remote sensing data to monitor mangroves and other coastal vegetation of India. *Indian Journals of Marine Science, 30*, 195-213.

5. Béland, M. G. (2006). Assessment of land-cover changes related to shrimp aquaculture using remote sensing data: A case in the Giao Thury District, Vietnam. *Int. J. Remote Sens*, 27, 1491-1510.

6. Berlanga-Robles, C. R.-L. (2002). Land use mapping and change detection in the coastal zone of northwest Mexico using remote sensing techniques. *J. Coast. Res*, 18, 514-522.

7. Blaschke, T. S. (2001). What's wrong with pixels? Some recent developments interfacing remote sensing and GIS. *GeoBIT/GIS*, 6, 12–17.

8. Brown, M. E., Pinzon, J. D., & C.J. (2006). Evaluation of the consistency of long-term NDVI time series derived from AVHRR, SPOT-Vegetation, SeaWiFS, MODIS, and Landsat ETM+ sensors. *Geoscience and Remote Sensing, IEEE Transactions on 44(7)*, 1787-1793.

9. Camile Sothe, C. M. (2017). Evaluating Sentinel-2 and Landsat-8 Data to Map Sucessional Forest Stages in a Subtropical Forest in Southern Brazil. *Remote Sens.*, 9, 838.

10. Campbell, J. B. (1987). *Introduction to Remote Sensing.* New York, US: The Guildford Press.

11. Claudia Kuenzer, A. B. (2011). Remote Sensing of Mangrove Ecosystems: A Review. *Remote Sensing*, 3, 878-928.

12. Congalton, R. G. (2001). Accuracy assessment and validation of remotely sensed and other spatial information. *International Journal of Wildland Fire, 10*.

13. Duke, N. (1992). Mangrove floristics and biogeography. In A. a. Robertson, *Tropical Mangrove Ecosystems, Coastal Estuarine Studies* (pp. 63–100). Washington, D.C: American Geophysical Union.

14. F. Blasco, T. G. (1998). Recent advances in mangrove studies using remote sensing data. *Marine and Freshwater Research*, 49: 287–96.

15. FAO (2007). *The World's Mangroves 1980-2005.* Rome, Italy: Food and Agriculture Organization of the United Nations.

16. Field, C., Osborn, J., Hoffmann, L., Polsenberg, J., Ackerly, D., Berry, J., Matson, P. a. (1998). Mangrove biodiversity and ecosystem function. *Global Ecology and Biogeography Letters*, 7, 3–14.

17. G.J. Hay, G. C. (2008). Geographic Object-Based Image Analysis (GEOBIA): A new name for a new discipline. In S. L. T. Blaschke, *Object Based Image Analysis* (pp. 93-112). Heidelberg, Berlin, New York: Springer.

18. Gao, J. (1998). Hybrid method toward accurate mapping of mangroves in a marginal habitat from SPOT Multispectral data. *Int. J. Remote Sens*, 19, 1887-1899.

19. Gilman, L., Ellison, J., & Duke, N. a. (2008). Threats to mangroves from climate change and adaptation options: a review. *Aquatic Botany*, 89(2), 237–250.

20. Giri, C. K. (1996). Assessing Land Use/Land Cover Dynamics in Two Identified ―Hot Spot‖ Areas: Oudomxay Province of Lao P.D.R. and Mekong Delta of Vietnam. *Proceeding of The 17th Asian Conference on Remote Sensing*, (pp. 4–8). Colombo, Sri Lanka.

21. Giri, C. P. (2007). Monitoring Mangrove forest dynamics of the Sundarbans in Bangladesh and India using multi-temporal satellite data from 1973 to 2000. *Estuar. Coast. Shelf Sci*, 73, 91-100.

22. Giri, M. J. (2008). Mangrove forest distribution and dynamics in Madagascar (1975–2005). *Sensors*, 8, 2104-2117.

23. Goodchild, M. F. (1994). Integrating GIS and remote sensing for vegetation analysis and modeling: methodological issues. *Journal of Vegetation Science*, 615-626.

24. Green, E. C. (1998). Remote sensing techniques for mangrove mapping. *Int. J. Remote Sens*, 19, 935-956.

25. Gross, D. (2005). Monitoring Agricultural Biomass Using NDVI Time Series. *Food and Agriculture Organization of the United Nations (FAO), Rome, Italy.*

26. H.Strahler, A. (1980). The use of prior probabilities in maximum likelihood classification of remotely sensed data. *Remote Sensing of Environment*, 10: 135-163.

27. Hankui K. Zhanga, D.C. (2018). Characterization of Sentinel-2A and Landsat-8 top of atmosphere, surface,and nadir BRDF adjusted reflectance and NDVI differences. *Remote Sensing of Environment 215*, 482 - 494.

28. Hernández Cornejo, R. K.G. (2005). Remote sensing and ethnobotanical assessment of the mangrove forest changes in the Navachiste-San Ignacio-Macapule Lagoon Complex, Sinaloa, Mexico. *Ecol. Soc.* , 10, art. 16.

29. Heumann, B. W. (2011). An Object-Based Classification of Mangroves Using a Hybrid Decision Tree—Support Vector Machine Approach. *Remote Sensing*, 3, 2440-2460.

30. Heumann, B. W. (2011). Satellite remote sensing of mangrove forests: recent advances and future opportunities. *Progress in Physical Geography, 35*, 87–108.

31. Horning, N. (2008). Remote Sensing. In S. Jorgensen, & B. Fath, *Encyclopedia of Ecology* (p. 2986). London: Elsevier Science.

32. Hu, Q (2013). Exploring the Use of Google Earth Imagery and Object-Based Methods in Land Use/Cover Mapping. *Remote Sensing, 5*, 6026-6042.

33. International Federation of Red Cross, R. C. (2009). *Mangrove plantation in Viet Nam: measuring impact and cost benefit.* Hanoi: ifrc.

34. Irons, J. D. (2012). The next Landsat satellite: the Landsat data continuity mission. *Remote Sens. Environment. 122*, 11 -21.

35. J.E. Sterling, M. H. (2006). Vietnam: a natural history. *Yale Univ. Press*, 1-21 and 91-92.

36. Kerrylee Rogers, L. L. (2017). Mapping of mangrove extent and zonation using high and low tide composites of Landsat data. *Hydrobiologia*.

37. Kirui, K. B. (2013). Mapping of mangrove forest land cover change along the Kenya coastline using Landsat imagery. *Ocean & Coastal Management*, 83, 19–24.

38. Knudby, A. L. (2014). Using multiple Landsat scenes in an ensemble classifier reduces classificlassification error in a stable nearshore environment. *International Journal of Applied Earth Observation and Geoinformation*, 28, 90–101.

39. Kovacs, J. M.-C. (2001). Mapping disturbances in a mangrove forest using multi-date Landsat TM imagery. *Environmental Management*, 27, 763–776.

40. Kuenzer, C. A. (2011). Remote sensing of mangrove ecosystems: a review. *Remote Sensing 3*, 878.

41. Kuenzer, C. A. (2011). Remote sensing of mangrove ecosystems: a review. *Remote Sensing 3*, 878.

42. L. Wang, W. P. (2004). imagery, Integration of object-based and pixel-based classification for mapping mangroves with IKONOS. *International Journal of Remote Sensing*, 25:24, 5655-5668.

43. L. X. Tuan, Y. M. (2003). Environmental Management in Mangrove. *Environmental Informatics Archives*, 1, 38-52.

44. Long, J. N. (2014). A mapping and monitoring assessment of the Philippines' mangrove forests from 1990 to 2010. *Journal of Coastal Research*, 30(2), 260–271.

45. Lu, D., Weng, Q. (2007). Survey of image classification methods and techniques for improving. *International Journal of Remote Sensing, 28, No. 5*, 823–870.

46. M. Drusch, U. D. (2012). Sentinel-2: ESA's optical high-resolution mission for GMES operational services. *Remote Sens. Environ., 120*, 25 - 36.

47. M. I. El-Gammal, R. R. (2014). NDVI Threshold Classification for Detecting Vegetation Cover in Damietta Governorate, Egypt. *American Science 10(8)*, 108-113.

48. Machado, S. E. (2002). Spatial temporal variability of sorghum grain yield: Influence of soil, water, pests, and diseases relationship. *Precise Agriculture*, 3: 389-406.

49. Manson, F. J. (2001). Assessing techniques for estimating the extent of mangroves: topographic maps, aerial photographs and Landsat TM images. *Marine and Freshwater Research 52*, 787–792.

50. Mavis, B. (2001). A socio-economic analysis of mangrove degradation in Samoa. *Geographical Review of Japan*, 74(2), 159–186.

51. Md. Mijanur Rahman (2013). Comparison of Landsat image classification methods for detecting mangrove forests in Sundarban. *International Journal of Remote Sensing, 34:4*, 1041-1056.

52. Md. Mijanur Rahmana, M. R. (2013). Comparison of Landsat image classification methods for detecting mangrove forests in Sundarban. *International Journal of Remote Sensing, 34, 4*, 1041–1056.

53. Minh Luu, D. O. (2014). Hydrological regime of a tidal system in the Red River Delta, northern Vietnam. *Hydrology in a Changing World: Environmental and Human Dimensions*, 363.

54. Neukermans, G. D.-G. (2008). Mangrove species and stand mapping in GAzi bay (Kenya) using Quickbird satellite imagery. *J. Spat. Sc*, 53, 75-86.

55. Nguyen Khanh Van, N. T. (2000). Bioclimatic charts of Vietnam. *Vietnam National University Press*.

56. Paul A Longley, M. F. (2005). *Geographic information systems and science.* John Wiley & Sons.

57. Phan Minh, J. P. (2007). Status and changes of mangrove forest in Mekong Delta. *Estuarine, Coastal and Shelf Science 71*, 98-109.

58. Phan Nguyen Hong, T. V. (1999). *Mangrove Forests of Vietnam.* Hanoi: Agriculture.

59. Phan Nguyen Hong, V. T. (2004). Some Natural feature of the mud flats in the coastal estuarine mangrove area of Thai Binh and Nam Dinh Provinces in Mangrove Ecosystem in the Red River Coastal Zone. *Agriculture Publishing House*, 1 - 15.

60. Primavera, J. 2. (2000). Development and conservation of Philippine mangroves: institutional issues. *Ecological Economics*, 35, 91–106.

61. Qiong Hu, W. W. (2013). Exploring the Use of Google Earth Imagery and Object-Based Methods in Land Use/Cover Mapping. *Remote Sensing, 5*, 6026-6042.

62. R. Kettig, D. L. (1976). Classification of multispectral image data by extraction and classification of homogeneous objects. *IEEE Transactions on Geoscience Electronics*, 19-26.

63. Ramsey, E. I., & Jensen, J. (1996). Remote sensing of mangrove wetlands: Relating canopy spectral to site-specific data. *Photogramm. Eng. Remote Sensing*, 62, 939-948.

64. Rasolofoharinoro, M. B. (1998). A remote sensing based methodology for mangrove studies in Madagascar. *Int. J. Remote Sens*, 19, 1873-1886.

65. Rasolofoharinoro, M. B. (1998). A remote sensing based methodology for mangrove studies in Madagascar. *Int. J. Remote Sens*, 19, 1873-1886.

66. Robert C. Weih, N. D. (2010). Object-based classification vs. Pixel-based classification: Comparitive importance of multi-resolution imagery.

67. Ruiz-Luna, A. B.-R. (1999). Modifications in coverage patterns and land use around the Huizache-Caimanero lagoon system, Sinaloa, Mexico: A multi-temporal analysis using Landsat images. *Estuar. Coast. Shelf Sci*, 49, 37-44.

68. Selvam, V. R. (2003). Assessment of community-based restoration of Pichavaram mangrove wetland using remote sensing data. *Curr. Sci*, 85, 794-798.

69. Seto K.C., F. M. (2007). Mangrove conversion and aquaculture development in Vietnam: A remote sensing-based approach for evaluating the Ramsar Convention on Wetlands. *Glob. Environ. Change*, 17, 486-500.

70. Shaban, M. A. (2001). Improvement of classification in urban areas by the use of textural features: the case study of Lucknow City, Uttar Pradesh. *International Journal of Remote Sensing*, 4, 565–593.

71. Shao, Y. L. (2012). Comparison of support vector machine, neural network, and CART algorithms for the land-cover classification using limited training data points. *ISPRS J.Photogramm. Remote Sens*, 70, 78–87.

72. Spalding, M. (1997). The global distribution and status of mangrove ecosystems. *Int. NewsLett. Coast.*, 1, 20-21.

73. Story M, C. R. (1986). Accuracy assessment: A user's perspective. *Photogrammetric Engineering and Remote Sensing, 52*, 397-299.

74. T.Blaschke. (2010). Object based image analysis for remote sensing. *ISPRS Journal of Photogrammetry and Remote Sensing*, 65, 2-16.

75. Thomas N, L. R. (2017). Distribution and drivers of global mangrove forest change, 1996–2010. *PLoS ONE, 12*, 6.

76. Thu, P. P. (2007). Status and changes of mangrove forest in Mekong Delta: Case study in Tra Vinh, Vietnam. *Estuar. Coast. Shelf Sci*, 71, 98-109.

77. Thuy Dang Truong, L. H. (2018). Mangrove forests and aquaculture in the Mekong river delta. *Land Use Policy*, 20-28.

78. Tomlinson, P. B. (1986). *The botany of mangroves.* Cambridge, England: Cambridge University Press.

79. Tong, P. A. (2004). Assessment from space of mangroves evolution in the Mekong Delta; in relation to extensive shrimp farming. *Int. J. Remote Sens* , 25, 4795-4812.

80. Trang Nguyen, L. Q. (2016). Object-Based vs. Pixel-Based Classification of Mangrove Forest Mapping in Vien An Dong Commune, Ngoc Hien District, Ca Mau Province Using VNREDSat-1 Images. *Advances in Remote Sensing*, 5, 284-295.

81. Umroha, W. A. (2016). Detection of Mangrove Distribution in Pongok Island. *Procedia Environmental Sciences 33*, 253 – 257.

82. Vaiphasa, C. O. (2005). Tropical mangrove species discrimination using hyperspectral data: A laboratory study. *Estuar. Coast. Shelf Sci*, 65, 371-379.

83. Vaiphasa, C. S. (2006). post-classifier for mangrove mapping using ecological data. *ISPRS J. Photogramm*, 61, 1-10.

84. Wang, L., Sousa, W., Gong, P., & Biging, G. (2004). Comparison of IKONOS and QuickBird imagery. *Remove Sensing Environment*, 91: 432-440.

85. Wolanski, E. M. (2015). Coastal Wetlands: An Integrated Ecosystem Approach. *The Netherlands*.

86. Xavier Ceamanos, S. V. (2017). Processing Hyperspectral Images. In M. Z. Nicolas Baghdadi, *Optical Remote Sensing of Land Surface* (p. 121). ISTE Press - Elsevier.

87. Xuehong Zhanga, P. M. (2017). Mapping mangrove forests using multi-tidal remotely-sensed data and a decision-tree-based procedure. *Int J Appl Earth Obs Geoinformation 67*, 201–214.

88. Young, N. E. (2017). A survival guide to Landsat preprocessing. *Ecology 98(4)*, 920 - 932.

89. Yu Q., G. P. (2006). Object-based detailed vegetation classification with airborne high spatial resolution remote sensing imagery. *Photogramm. Eng. Remote Sens*, 72, 799–811.

90. Yuehong Chen, Y. Z. (2018). Enhancing Land Cover Mapping through Integration of Pixel-Based and Object-Based Classifications from Remotely Sensed Imagery. *Remote Sensing*, 10, 77.

APPENDIX

Appendix 1: GPS fieldwork sheet

ID	Coordinates		Land Use/ Land Cover
	X	**Y**	**Type**
1	106.02100000000	19.96160000000	Mangrove
2	106.03800000000	19.95250000000	Mangrove
3	106.02000000000	19.95900000000	Mangrove
4	106.04400000000	19.93710000000	Non-Mangrove
5	106.05600000000	19.93130000000	Mangrove
6	106.05400000000	19.93380000000	Mangrove
7	106.05200000000	19.93880000000	Mangrove
8	106.05600000000	19.92740000000	Non-Mangrove
9	106.04600000000	19.93390000000	Non-Mangrove
10	106.05400000000	19.93480000000	Mangrove
11	106.04700000000	19.94990000000	Mangrove
12	106.02300000000	19.95720000000	Non-Mangrove
13	106.04100000000	19.95210000000	Mangrove
14	106.03700000000	19.95870000000	Mangrove
15	106.03800000000	19.95500000000	Mangrove
16	106.04700000000	19.94710000000	Non-Mangrove
17	106.03200000000	19.95350000000	Non-Mangrove
18	106.04800000000	19.94330000000	Mangrove
19	106.01800000000	19.95830000000	Mangrove
20	106.02600000000	19.96000000000	Non-Mangrove
21	106.03000000000	19.95530000000	Mangrove
22	106.03600000000	19.95880000000	Mangrove
23	106.03500000000	19.95600000000	Mangrove
24	106.03400000000	19.95990000000	Mangrove
25	106.06400000000	19.91790000000	Mangrove
26	106.05000000000	19.94200000000	Mangrove
27	106.04500000000	19.94000000000	Mangrove

28	106.03400000000	19.96030000000	Mangrove
29	106.05500000000	19.93570000000	Mangrove
30	106.03200000000	19.95430000000	Non-Mangrove
31	106.03200000000	19.95990000000	Mangrove
32	106.07100000000	19.91700000000	Mangrove
33	106.04800000000	19.93460000000	Mangrove
34	106.06300000000	19.91860000000	Non-Mangrove
35	106.07100000000	19.91870000000	Mangrove
36	106.03200000000	19.96030000000	Non-Mangrove
37	106.04900000000	19.93300000000	Mangrove
38	106.04600000000	19.93470000000	Mangrove
39	106.03400000000	19.95600000000	Mangrove
40	106.02900000000	19.95870000000	Mangrove
41	106.02500000000	19.96480000000	Mangrove
42	106.03500000000	19.95610000000	Mangrove
43	106.04800000000	19.94800000000	Mangrove
44	106.05600000000	19.93450000000	Mangrove
45	106.03800000000	19.95180000000	Mangrove
46	106.06500000000	19.91990000000	Mangrove
47	106.04300000000	19.94340000000	Mangrove
48	106.04900000000	19.93180000000	Non-Mangrove
49	106.04500000000	19.95090000000	Non-Mangrove
50	106.03400000000	19.95510000000	Mangrove
51	106.04100000000	19.94560000000	Mangrove
52	106.02200000000	19.95850000000	Mangrove
53	106.05300000000	19.93870000000	Mangrove
54	106.06800000000	19.92040000000	Mangrove
55	106.06600000000	19.91790000000	Non-Mangrove
56	106.05300000000	19.93170000000	Mangrove
57	106.04300000000	19.94120000000	Mangrove
58	106.04800000000	19.93360000000	Mangrove
59	106.03600000000	19.95310000000	Mangrove
60	106.04300000000	19.94930000000	Non-Mangrove

61	106.04800000000	19.94160000000	Non-Mangrove
62	106.03900000000	19.95130000000	Mangrove
63	106.03600000000	19.95220000000	Mangrove
64	106.03300000000	19.95340000000	Mangrove
65	106.03100000000	19.95610000000	Mangrove
66	106.03500000000	19.95330000000	Mangrove
67	106.05300000000	19.92980000000	Mangrove
68	106.02200000000	19.95830000000	Mangrove
69	106.06200000000	19.92060000000	Non-Mangrove
70	106.04800000000	19.93540000000	Mangrove
71	106.04900000000	19.94300000000	Non-Mangrove
72	106.05500000000	19.93710000000	Non-Mangrove
73	106.04700000000	19.93840000000	Mangrove
74	106.02400000000	19.96370000000	Non-Mangrove
75	106.05300000000	19.93260000000	Non-Mangrove
76	106.06700000000	19.91970000000	Non-Mangrove
77	106.04100000000	19.94830000000	Mangrove
78	106.05700000000	19.93350000000	Mangrove
79	106.06700000000	19.91680000000	Non-Mangrove
80	106.02100000000	19.96070000000	Non-Mangrove
81	106.03400000000	19.95380000000	Non-Mangrove
82	106.06500000000	19.92080000000	Mangrove
83	106.02200000000	19.96230000000	Non-Mangrove
84	106.04500000000	19.94730000000	Non-Mangrove
85	106.05300000000	19.93600000000	Mangrove
86	106.05100000000	19.93250000000	Non-Mangrove
87	106.05200000000	19.94690000000	Mangrove
88	106.05000000000	19.93650000000	Mangrove
89	106.03500000000	19.95330000000	Non-Mangrove
90	106.05000000000	19.94140000000	Mangrove
91	106.03700000000	19.95240000000	Mangrove
92	106.05900000000	19.92440000000	Mangrove
93	106.05000000000	19.94020000000	Mangrove

94	106.03800000000	19.95040000000	Mangrove
95	106.07000000000	19.91810000000	Mangrove
96	106.06200000000	19.91930000000	Non-Mangrove
97	106.03000000000	19.95930000000	Non-Mangrove
98	106.02700000000	19.95700000000	Non-Mangrove
99	106.05900000000	19.92380000000	Mangrove
100	106.02000000000	19.95850000000	Non-Mangrove

Appendix 2: Fieldwork

Mangrove forest in Ninh Binh province during relatively spring tide *(04/07/2019)*

Using GPS device to assess classification accuracy during field work *(05/07/2019)*

Aqua-culture area nearby mangrove forest in Ninh Binh Province *(15/06/2019)*

Bare land cover at mangrove forest in Ninh Binh province (15/06/2019)